



# Ammonia exchange flux over a tropical dry deciduous forest in the dry season in Thailand

Mao Xu<sup>1,2</sup>, Phuvasa Chanonmuang<sup>3</sup>, Hiroyuki Sase<sup>4</sup>, Atsuyuki Sorimachi<sup>5</sup>, Syuichi Itahashi<sup>2</sup>, Kazuhide Matsuda<sup>6</sup>

5 <sup>1</sup>Institute of Global Innovation Research, Tokyo University of Agriculture and Technology, Fuchu, Tokyo, 183-8538, Japan

<sup>2</sup>Research Institute for Applied Mechanics, Kyushu University, Kasuga, Fukuoka 816-8580, Japan

<sup>3</sup>Thailand Institute of Scientific and Technological Research, Khlong Luang, Pathum Thani 12120, Thailand

<sup>4</sup>Asia Center for Air Pollution Research, Niigata, Niigata 950-2144, Japan

<sup>5</sup>Toyo University, Kawagoe, Saitama 350-8585, Japan

10 <sup>6</sup>Faculty of Agriculture Field Science Center, Tokyo University of Agriculture and Technology, Fuchu, Tokyo, 183-8509, Japan

*Correspondence to:* Mao Xu (maoxu@riam.kyushu-u.ac.jp), Kazuhide Matsuda (kmatsuda@cc.tuat.ac.jp)

**Abstract.** Ammonia (NH<sub>3</sub>) is a significant contributor to total nitrogen deposition in East Asia. However, process-based observations that specifically focus on the air–surface exchange of NH<sub>3</sub> remain limited in this region, especially in Southeast Asia. To clarify the bi-directional exchange process of NH<sub>3</sub> under tropical climatic conditions, we first observed the NH<sub>3</sub> exchange flux over a tropical dry deciduous forest in Thailand during two periods with different canopy and meteorological conditions in the dry season using the aerodynamic gradient method. NH<sub>3</sub> concentrations exhibited strong positive correlations with air temperature and negative correlations with wind speed during the first half of the observation period. However, there was no clear correlation between concentrations and meteorological elements during the second half. Measured NH<sub>3</sub> fluxes fell within the ranges presented in recent studies, with a weighted mean and standard deviation of  $0.148 \pm 0.240 \mu\text{g m}^{-2} \text{s}^{-1}$ , and consistently larger during daytime. During the dry season, the tropical dry deciduous forest acted as an emission source of NH<sub>3</sub>. Across both observation periods, NH<sub>3</sub> emissions were governed by air temperature, relative humidity, friction velocity, and solar radiation. While no clear difference in fluxes magnitude was observed between the first half ( $0.140 \pm 0.240 \mu\text{g m}^{-2} \text{s}^{-1}$ ) and the second half ( $0.158 \pm 0.239 \mu\text{g m}^{-2} \text{s}^{-1}$ ), the main source of NH<sub>3</sub> emission in the tropical dry deciduous forest probably shifted dynamically from stomata to leaf litter due to the changes in meteorological, canopy, and forest floor conditions.

## 1 Introduction

Nitrogen is an essential element for humans and has significantly benefited agriculture and manufacturing (Hayashi et al., 2021). However, the excessive use of nitrogen places a heavy burden on the environment, causing climate change, air and water pollution, acidification, eutrophication, and biodiversity loss through atmospheric deposition (Kuriyama and Hayashi; Nishina et al., 2017). Concerns about nitrogen-related issues are growing on a global scale, as evidenced by the adoption of a



resolution on "sustainable nitrogen management" in the Fifth session of the United Nations Environment Assembly in 2022 (Nishina et al., 2025). The world is currently under pressure to develop plans to reduce nitrogen emissions, but outside of Western countries, where reports on nitrogen assessment (EPA, 2011; Sutton et al., 2011) have already been published, there is limited knowledge about nitrogen dynamics and assessments needed for its management (Rudek et al., 2017).

East Asia is one of the regions at high risk of nitrogen pollution and is a hotspot for nitrogen deposition (Rubin et al., 2023; Nishina et al., 2021). In this region, the Acid Deposition Monitoring Network in East Asia (EANET), an intergovernmental network that began full-scale operation in January 2001, is currently monitoring air concentrations and atmospheric deposition of pollutants at 65 sites in 13 countries (EANET, 2024). To date, estimations of nitrogen deposition on a national scale have been conducted mainly in Japan (Chatani et al., 2025; Yamaga et al., 2021; Ban et al., 2016; Endo et al., 2011) and China (Chen et al., 2023; Zhou et al., 2023; Wen et al., 2020) using data from the EANET and/or the nitrogen monitoring network in China. These studies have revealed that the dry deposition of  $\text{NH}_3$ , which is the main reduced form of nitrogen, has increased significantly among total nitrogen depositions, following dramatic changes in nitrogen oxides emissions in recent years. The model-based approach may contain uncertainties; therefore, process-based observations were conducted at several sites to verify model performance and improve the accuracy of the deposition estimates. Observational data on the main components contributing to nitrogen deposition, including  $\text{NH}_3$ , have been gathered from Japanese forests (Xu et al., 2024; Wu et al., 2024; Xu et al., 2023; Xu et al., 2021, Xu and Matsuda, 2020, Nakahara et al., 2019, Hayashi et al., 2011) and agricultural fields (Xu et al., 2022, Hayashi et al., 2017; Hayashi et al., 2012) located in temperate and cool temperate zones, and  $\text{NH}_3$  flux observations are now being carried out in Chinese agricultural fields (Wang et al., 2021).

Despite evidence that forests in Southeast Asian countries are exposed to high nitrogen deposition (Ban et al., 2022) and that deposition amounts often exceed the critical load for eutrophication (Yamashita et al., 2022), national-scale estimates of nitrogen deposition remain limited in many of these countries (Beachley et al., 2024). Moreover, process-based observations have only been conducted for sulfur compounds, ozone, and elemental carbon at some forest sites in Thailand (Chanonmuang et al., 2015; Khoomsab et al., 2014; Matsuda et al., 2012; Matsuda et al., 2006; Matsuda et al., 2005), whereas studies specifically focusing on nitrogen deposition are comparatively limited. Understanding the behavior of major nitrogen compounds, particularly the air-surface exchange of  $\text{NH}_3$ , in tropical climates which differ significantly from those of Japan and China is essential for improving the accuracy of deposition estimates in East Asia through model advancement. This will also help address key scientific questions related to nitrogen cycle in diverse regions. Against this backdrop, we performed the world's first observation of  $\text{NH}_3$  exchange flux over a tropical dry deciduous forest in Thailand. Measurements were taken during two periods in the dry season, which differed in environmental conditions: (i) rising air temperatures as the season progressed and (ii) substantial leaf fall, which significantly altered canopy and forest floor conditions. As shown in Saylor et al. (2025) who summarized previous studies until recently, the behavior of  $\text{NH}_3$  depends on many factors (e.g.  $\text{NH}_3$  concentration, canopy condition, the presence of source, meteorological, and soil elements) and varies from one study site to another, making it difficult to generalize the exchange process. Therefore, our first step was to understand the



65 characteristics of the exchange process in tropical deciduous forests by measuring  $\text{NH}_3$  fluxes and meteorological elements  
and clarifying their relationships.

## 2 Methodology

### 2.1 Site description

We conducted the observation in the forest of Sakaerat Environmental Research Station (SERS), Nakhon Ratchasima  
70 Province, Thailand ( $14^\circ 30' \text{ N}$ ,  $101^\circ 55' \text{ E}$ ), as shown in Fig. 1. SERS is the core area of the Sakaerat Biosphere Reserve,  
which was the first biosphere reserve in Thailand recognized for its rich biodiversity of flora and fauna. According to the  
Köppen climate classification, SERS is classified as a tropical savanna, with annual mean air temperature of  $24.9^\circ \text{ C}$  and  
annual rainfall of 1472 mm during the 3 years from 2020 to 2022 (Fig. 2). SERS is characterized by high temperatures  
throughout the year and distinct wet (April to October) and dry (November to March) seasons (Matsuda et al, 2012). From  
75 December to February, the dry season is especially pronounced, with a monthly rainfall of less than 50 mm (Sase et al.,  
2017; Sase et al., 2012). The forest of SERS consists of dry evergreen and dry deciduous forests (DDF) (Murata et al. 2009).  
We used a 38 m walk-up observation tower installed in the DDF located near the northeastern edge of the SERS. The DDF is  
almost flat and sparse, and Dipterocarps such as *Shorea obtusa* and *Shorea siamensis* dominate in the area around the tower  
(Murata et al. 2011), with a canopy height ( $h$ ) of about 20 m. Leaf area index (LAI) around the observation tower measured  
80 by a plant canopy analyzer (LI-COR LAI-2200) at the beginning of the observation was in the range from 2.5 to 4.2 with a  
mean value of 3.1. Although the eastern side of SERS is mainly covered by agricultural fields and residential areas, the  
observation tower is located at least 400 m away from these areas. Further details regarding the topography and seasonal  
variations in leaf conditions of the DDF are described in Matsuda et al. (2012).

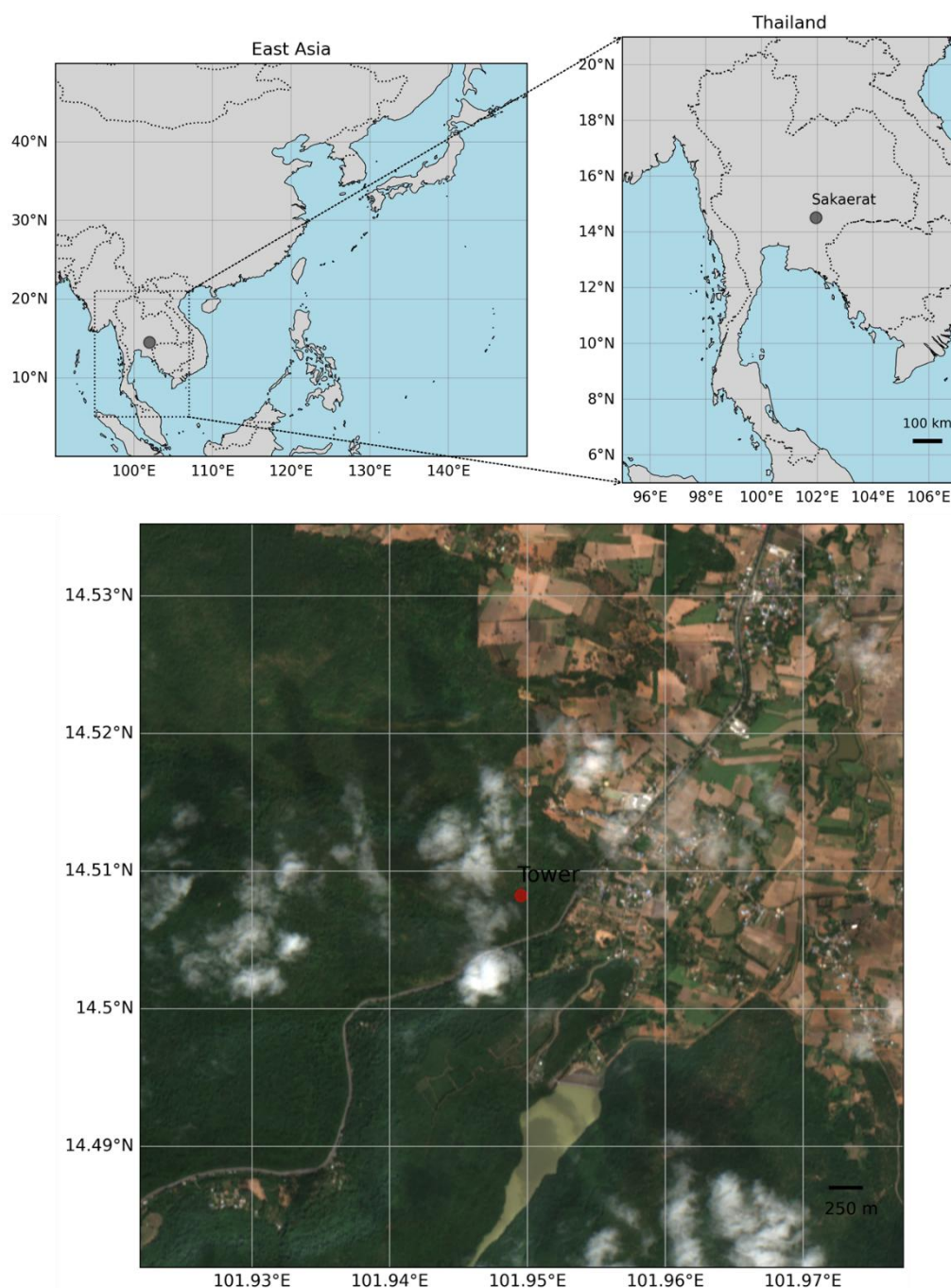


**Figure 1: Location and surrounding environment of the observation site (gray circle) and tower (red circle) in the Sakaerat Environmental Research Station. Satellite imagery (6 km × 6 km) was retrieved from the dataset of Sentinel-2 Surface Reflectance Harmonized (COPERNICUS/S2\_SR\_HARMONIZED) via © Google Earth Engine. The data was filtered for the observation point, and date from December 15 to December 31, 2023, with a cloud cover percentage of less than 20% was shown.**

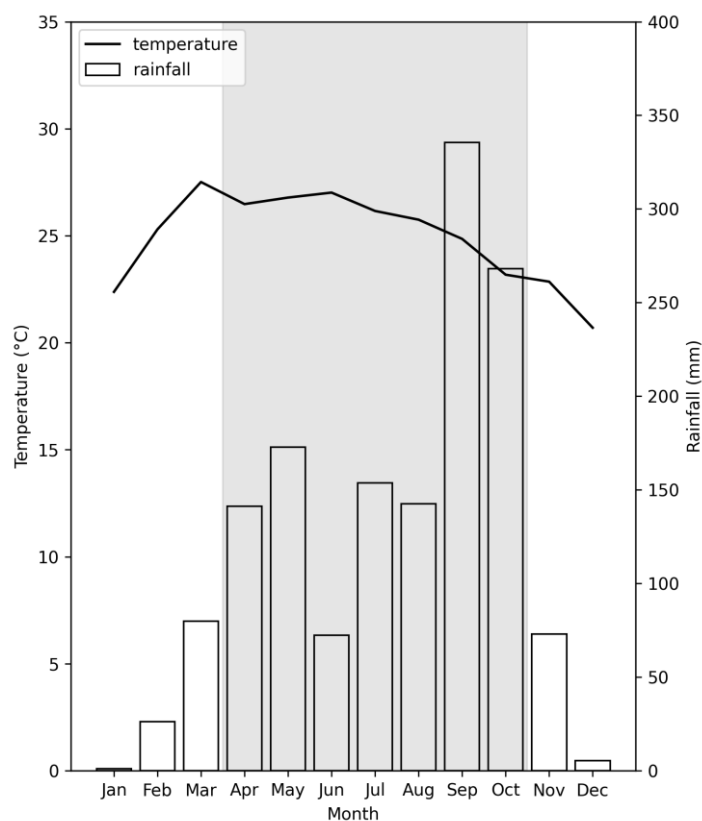


**Figure 2: Variations in monthly mean air temperature (line) and rainfall (bar) at the weather station of Sakaerat Environmental Research Station based on the meteorological data recorded from January 2020 to December 2022. Gray hatch indicates the wet season (from April to October).**

95

## 2.2 Flux measurements for ammonia using aerodynamic gradient method

We measured  $\text{NH}_3$  fluxes using the aerodynamic gradient method (AGM), which is a globally recognized method for determining trace gas fluxes (Melman et al., 2025, Xu et al., 2023), over the DDF of SERS. The observation periods were from 15 December 2023 to 30 December 2023 (hereinafter referred to “first half”), and from 22 January 2024 to 6 February 2024 (“second half”). To avoid duplication, we briefly describe the AGM theory. Using the AGM, the flux ( $F$ ) can be calculated by multiplying the turbulent diffusivity by the vertical gradient of concentration according to Fick’s law:

$$F = -D\Delta C \quad (1)$$

where  $D$  is the transfer velocity, and  $\Delta C$  is the concentration difference between two heights of  $z_1$  and  $z_2$  ( $z_2 > z_1$ ) above the canopy (Matsuda et al., 2010). We obtained transfer velocity from micrometeorological elements (i.g. the friction velocity and the Monin–Obukhov length) recorded by a 3D sonic anemometer (YOUNG, 81000) installed at the height of 31.5 m at the observation tower and the displacement height ( $d$ ) following Xu et al. (2023) and Matsuda et al. (2010). Matsuda et al.

100

105



(2012) derived seasonal  $d$  for the DDF of SERS from the relationship between friction velocity and wind speed, and the relationship between  $d/h$  and LAI; 0.7 for the leafy season and 0.6 for the transitional season, respectively. We also determined  $d$  from the relationship between friction velocity and wind speed, and the values obtained were the same as those of Matsuda et al. (2012); 0.7 for the first half and 0.6 for the second half of the observation period, respectively.

We derived  $\Delta C$  from the  $\text{NH}_3$  concentration measured at heights of 34 m ( $z_2$ ) and 26 m ( $z_1$ ) at the observation tower using the filter-pack holders (Tokyo Dylec Corporation, NILU filter folder NL-O) which consist of four stages. This system is the same as that used by Xu et al. (2023).  $\text{NH}_3$  was collected at the last stage of the filter-pack holder by using a phosphoric acid impregnated cellulose filter with a flow rate of  $20 \text{ L min}^{-1}$ . We continuously collected two daytime (D1: 9:00–13:00, D2: 13:00–17:00) and one nighttime (N: 17:00–9:00) samples (three samples per day) for 15 days each in the first and second halves of the observation period. After sampling, the ammonium ions in each cellulose filter were extracted into deionized water (10 ml) using an ultrasonic method, and were analyzed using two ion chromatographs (Dionex, ICS-1100 and Shimadzu Corp., HIC-ESP) for quality control. The  $\text{NH}_3$  concentrations obtained were almost the same; however, those of ICS-1100 tended to be slightly higher. Since the HIC-ESP had a better calibration curve for ammonium ions than the ICS-1100, its analytical results were adopted. We also performed laboratory ( $n = 5$ ) and travel ( $n = 5$ ) blank tests. We subtracted the median value of travel blanks when calculating  $\text{NH}_3$  concentrations because the ammonium content was higher in the travel blanks than in the laboratory blanks.

## 2.3 Meteorological measurements

We recorded wind speed, wind direction, and other elements to calculate the transfer velocity using a 3D sonic anemometer (YOUNG, 81000) installed at 31.5 m at the observation tower. We also recorded the air temperature and relative humidity at 34 m and 26 m at the observation tower using a thermometer (T&D Corp., TR-73 U). All elements were recorded at 10-min intervals. Observations of meteorological elements were also conducted by SERS in a vacant lot approximately 1.2 km west of the observation tower, and we used 1-h values of solar radiation and rainfall recorded at this weather station. Rainfall did not occur during the observation period.

## 3 Results and discussion

### 3.1 Variations in ammonia concentration

The temporal variations in  $\text{NH}_3$  concentrations at 34 m and 26 m during the observation period are shown in Fig. 3. Of the 90 samples we collected, two samples were missing owing to the problems in the electrical system and eight samples overlapped with the forest fire period described later in the second half; approximately 89% of the total samples were valid. All valid samples exceeded the limit of quantification (10 times the standard deviation of travel blanks). Variations in the  $\text{NH}_3$  concentrations were clearly different between the first and second halves of the observation period. In the first half,  $\text{NH}_3$  concentration at 34 m ranged from 1.06 to  $5.25 \mu\text{g m}^{-3}$ , and gradually decreased toward the middle of the period and then





increased again. The  $\text{NH}_3$  concentration at 26 m exhibited a similar variation to that at 34 m. The weighted means with standard deviations of  $\text{NH}_3$  concentration by sampling time at 34 m and 26 m were  $2.69 \pm 0.93 \mu\text{g m}^{-3}$  and  $2.88 \pm 0.95 \mu\text{g m}^{-3}$ , respectively.

In the second half, a large-scale forest fire occurred around the observation tower from the morning of 3 February. According to Ishida et al. (2023), forest fires frequently occur during the late dry season (from January to March) in the DDF of SERS. During the forest fire period,  $\text{NH}_3$  concentrations peaked at D2 on 3 February ( $106.81 \mu\text{g m}^{-3}$  at 26 m) and then drastically decreased to below  $10 \mu\text{g m}^{-3}$  after 3 February. Because this period was far from typical conditions, we excluded the data from subsequent analysis. Data from the forest fire period will be presented in a follow-up study. Excluding samples during the forest fire,  $\text{NH}_3$  concentration at 34 m ranged from  $1.24$  to  $4.36 \mu\text{g m}^{-3}$ . The concentrations at 34 m did not change until the middle of the period and decreased to below  $2 \mu\text{g m}^{-3}$  before the period of the forest fire. As in the first half, the concentration at 26 m showed a similar variation to that at 34 m. The weighted means and standard deviations of  $\text{NH}_3$  concentration by sampling time at 34 m and 26 m were  $2.96 \pm 0.75 \mu\text{g m}^{-3}$  and  $3.17 \pm 0.75 \mu\text{g m}^{-3}$ , respectively. The mean concentration was slightly higher at both measurement heights during the second half.

In both periods, the concentrations at 26 m tended to be higher than those at 34 m, particularly during the daytime. The differences in the concentration were on average  $0.51 \mu\text{g m}^{-3}$  at D1 (from 9:00 to 13:00) and  $0.41 \mu\text{g m}^{-3}$  at D2 (from 13:00 to 17:00) in the first half, and were on average  $0.36 \mu\text{g m}^{-3}$  at D1 and  $0.33 \mu\text{g m}^{-3}$  at D2 in the second half. Although the concentration variations differed between the two observation periods, a consistent tendency of higher concentrations was observed at 26 m than at 34 m during the daytime. These results suggest the possibility of daytime  $\text{NH}_3$  emissions from the DDF. However, this tendency was not pronounced at nighttime in either period, and there were also cases where the concentration at 34 m was higher than that at 26 m.

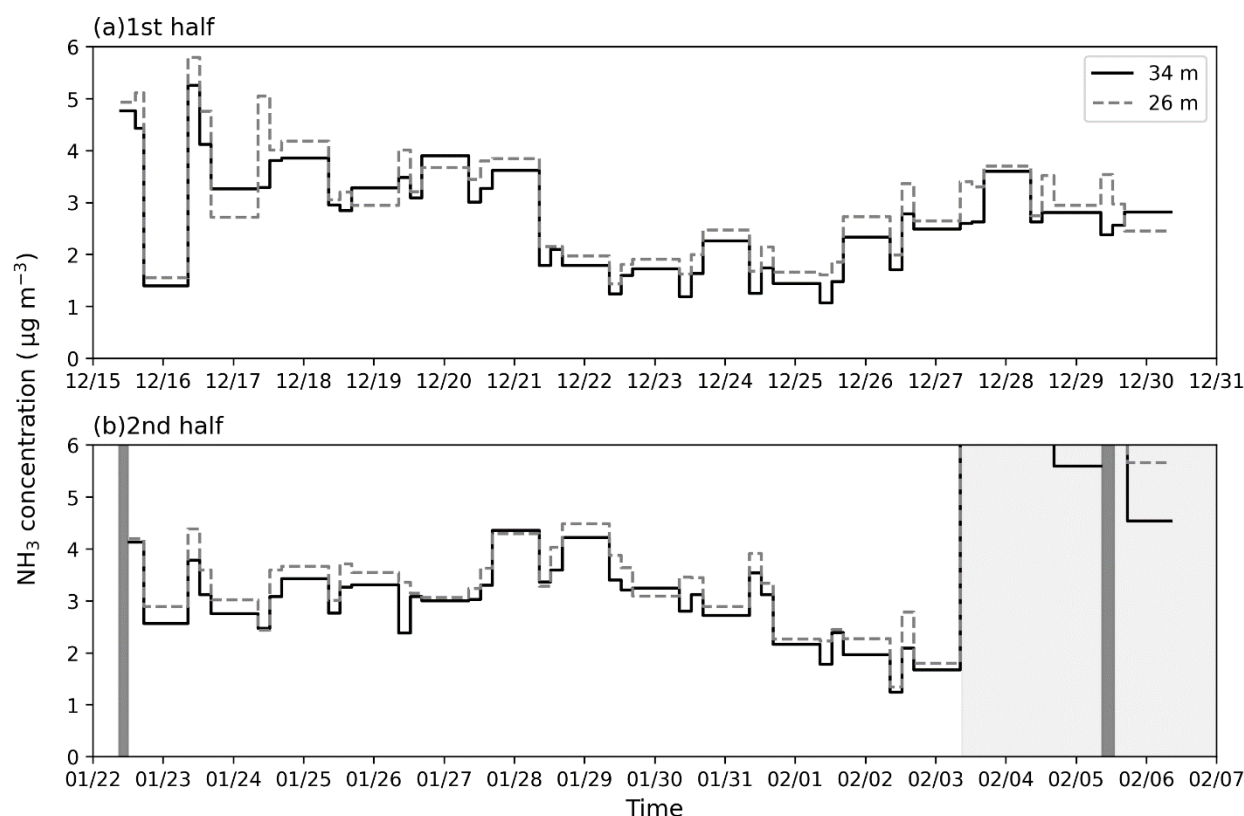


**Figure 3: Temporal variations in  $\text{NH}_3$  concentration at 34 m (solid line) and 26 m (dashed line) during (a) the first half and (b) second half of the observation periods. The length of line indicates the duration of sampling. Gray hatches indicate missing data, and light gray hatch indicates the high concentration period during and after the forest fire around the observation tower. Data during the forest fire periods was not included in the analysis of this study. The range of concentration for the second half is aligned for the figure visibility.**

Approximately 7 km southwest of our observation site, EANET had a monitoring site at the Sakaerat Silvicultural Research Station (SRS). At the SRS,  $\text{NH}_3$  concentrations were measured at 10-day intervals using the filter pack method from 2006 until its closure in 2020 (EANET, 2021). Although there are several missing data, which is inevitable in such long-term monitoring, the annual mean concentration of  $\text{NH}_3$  over the 5-years from 2015 to 2019 ranged from 2.5 to 4.1  $\mu\text{g m}^{-3}$ . The mean concentration obtained during the observation period was within this range, suggesting that our observations had a certain degree of reliability. In addition, the  $\text{NH}_3$  concentration levels at the SERS site were in a high category compared to those at various forest sites reported in papers published after the 2010s (Melman et al, 2025; Walker et al., 2023; Xu et al., 2023; Ramsay et al., 2020).





### 3.2 Factors controlling ammonia concentration

175 The hourly variations in the meteorological elements during the observation period are shown in Fig. 4. Like the variations  
in  $\text{NH}_3$  concentration, the air temperature showed a clear difference between the first and second halves of the observation  
period. During the first half, the temperature followed the same trend as the  $\text{NH}_3$  concentration. It decreased towards the  
middle of the period, and then increased again. In the second half, there was a gradual increase in temperature after 24  
January. The ranges and means with standard deviations of temperatures at 34 m were from 12.6 to 32.2 °C and  $22.7 \pm$   
180  $4.2$  °C in the first half, and were from 16.5 to 35.5 °C and  $25.6 \pm 3.9$  °C in the second half, respectively. There was no  
obvious variation in the relative humidity. The ranges and means with standard deviations of relative humidity at 34 m were  
from 40.2 to 90 % and  $63.7 \pm 12.4$  % in the first half, and were from 31.3 to 87.5 % and  $61.0 \pm 12.7$  % in the second half,  
respectively. The wind speed showed an inverse variation with temperature in the first half of the period and showed an  
increase at the end of the second half. The ranges and means with standard deviations of wind speed at 31.5 m were from 0.4  
185 to  $5.2 \text{ m s}^{-1}$  and  $2.5 \pm 0.9 \text{ m s}^{-1}$  in the first half, and were from 0.5 to  $5.5 \text{ m s}^{-1}$  and  $2.4 \pm 0.9 \text{ m s}^{-1}$  in the second half,  
respectively. During the first half, the main wind direction was northeasterly, with intermittent southwesterly winds  
occurring at nighttime. On the other hand, during the second half, the daytime wind direction shifted from northeasterly to  
southwesterly from 1 February. At nighttime, wind direction was mainly southwesterly except for four days between the  
beginning and middle of this period. The windrose during the observation period is shown in Fig. A1. The differences in the  
190 variations in temperature, wind speed and wind direction were thought to be related to the differences in the concentration  
variations between the first and second halves of the observation period.

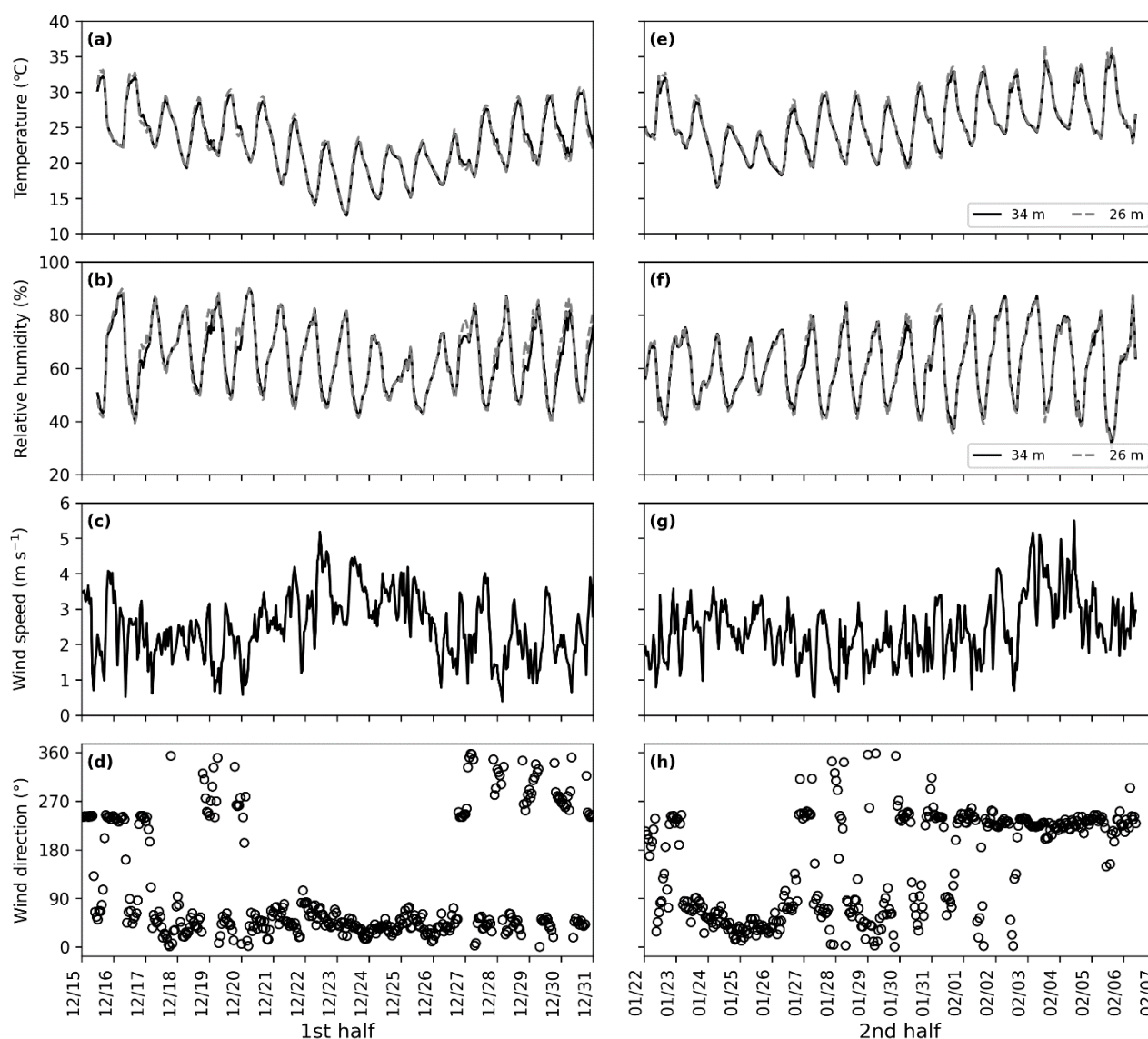


**Figure 4: Hourly variations in air temperature, relative humidity, wind speed, and wind direction during the first half ((a), (b), (c), (d)) and second half ((e), (f), (g), (h)) of the observation periods. Air temperature and relative humidity were recorded at 34 m (solid line) and 26 m (dashed line), and wind speed and wind direction were recorded at 31.5 m of the observation tower, respectively.**

The relationships between the  $\text{NH}_3$  concentration and air temperature, relative humidity, and wind speed during the first half of the observation period are shown in Fig. 5. The relationships between the concentrations at 34 m and 26 m and meteorological elements were roughly the same.  $\text{NH}_3$  concentrations showed strong positive correlations with temperature, especially during the D1 and D2; the correlation coefficients at 34 m were 0.97 and 0.89, respectively. In the 1-year vertical



profile measurements at a Japanese deciduous forest using the denuder method, Xu et al. (2024) revealed that  $\text{NH}_3$  concentrations near the forest floor showed strong positive correlations with temperature on a weekly basis during the leafy period ( $\text{LAI} = 2.3\sim 4.1$ ). Osada (2020) measured hourly  $\text{NH}_3$  concentrations using a semi-continuous microflow analytical system in a Japanese urban area and found that daily  $\text{NH}_3$  concentrations have a strong relationship with the magnitude of temperature and may be affected by different processes during the daytime and nighttime. Our observations revealed that daytime  $\text{NH}_3$  concentrations were strongly controlled by temperature in the tropical DDF of Thailand, even at the shorter timescale of 4-h. Furthermore, the weaker correlation at nighttime ( $R = 0.60$  at 34 m and  $R = 0.44$  at 26 m) also indicates that the process controlling concentrations might change between daytime and nighttime.  $\text{NH}_3$  concentrations also showed negative correlations with wind speed during each sampling time; the correlation coefficients at 34 m were  $-0.75$  (D1),  $-0.73$  (D2), and  $-0.76$  (N), respectively. This means that  $\text{NH}_3$  over the forest was dispersed when the wind speed was high and remained when the wind speed was low. While relative humidity ranged widely from 40% to 80%, no conspicuous correlation was found with  $\text{NH}_3$  concentration, suggesting that it was not the main factor controlling  $\text{NH}_3$  concentration in the DDF.

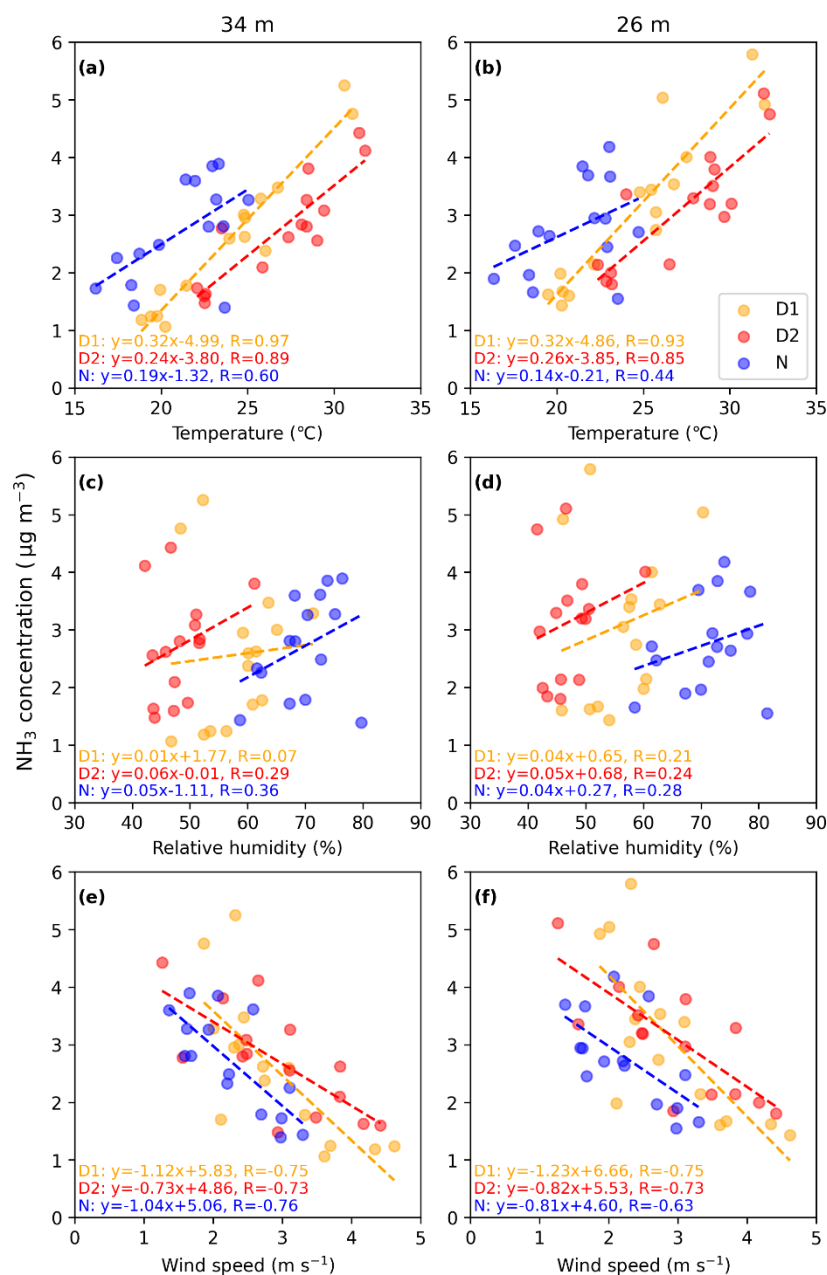


**Figure 5: Relationship between NH<sub>3</sub> concentration at each height (34 m: (a), (c), (e); 26 m: (b), (d), (f)) and air temperature, relative humidity, and wind speed during the first half. Air temperature and relative humidity were recorded at 34 m ((a), (c)) and 26 m ((b), (d)), and wind speed was recorded at 31.5 m of the observation tower.**

On the other hand, there was no clear correlation between the concentrations at 34 m and 26 m and the meteorological elements during each sampling time in the second half (Fig. 6), as can be seen in the first half (Fig. 5). Surprisingly, there



seemed to be an opposite relationship, indicating that the concentration decreases with an increase in temperature at  
225 nighttime. This was possibly due to the change in wind direction (from northeast to southwest) in the second half, as  
mentioned above. In fact, the opposite relationship disappeared after excluding data from 1 February, and concentrations at  
34 m and 26 m showed a positive correlation with temperature during D1 ( $R = 0.57, 0.59$ ). Moreover, the opposite nighttime  
relationship, which showed a decrease in concentration associated with increases in temperature and relative humidity, was  
less noticeable.

230 In addition to the change in wind direction, leaf fall occurred in the DDF of SERS from the end of the first half of the  
observation period to the end of the second half (Fig. A2). The satellite-derived LAI at the observation tower from the  
dataset of MCD15A3H, which is a product of the Moderate Resolution Imaging Spectroradiometer onboard the Terra and  
Aqua satellites (Myneni et al., 2015), is shown in Fig. A3. The LAI values, 4-day composite data with a spatial resolution of  
500 m, were obtained from the combined observations of both satellites. Based on the quality control of MCD15A3H, all  
235 data during the period were evaluated as best result possible with highest confidence. The satellite-derived LAI was  
approximately 3 at the beginning of the first half, which is close to the observed mean value around the observation tower.  
The LAI was halved just before the beginning of the second half of the observation period and was less than 1 at the end of  
the campaign. In addition, as can be seen from satellite images (Fig. A4) taken during the observation period, defoliation  
progressed not only around the tower but also throughout the entire DDF of SERS in approximately 20 days from 1 January  
240 2024 to 21 January 2024. Considering that the concentrations at 34 m in the first half had correlations with air temperature  
( $R = 0.70$ ) and wind speed ( $R = -0.69$ ) in total, the concentrations in the second half were probably governed by different  
process. This process may have been driven by structural changes in the forest due to substantial leaf fall, rather than by  
changes in meteorological conditions alone. Similarly, Xu et al. (2024) found that the strong correlation between  $\text{NH}_3$   
concentration and temperature observed during the leafy period was no longer observed during the leafless period ( $\text{LAI} <$   
245 1.5), also suggesting that concentration may be controlled by factors other than temperature during the leafless period.

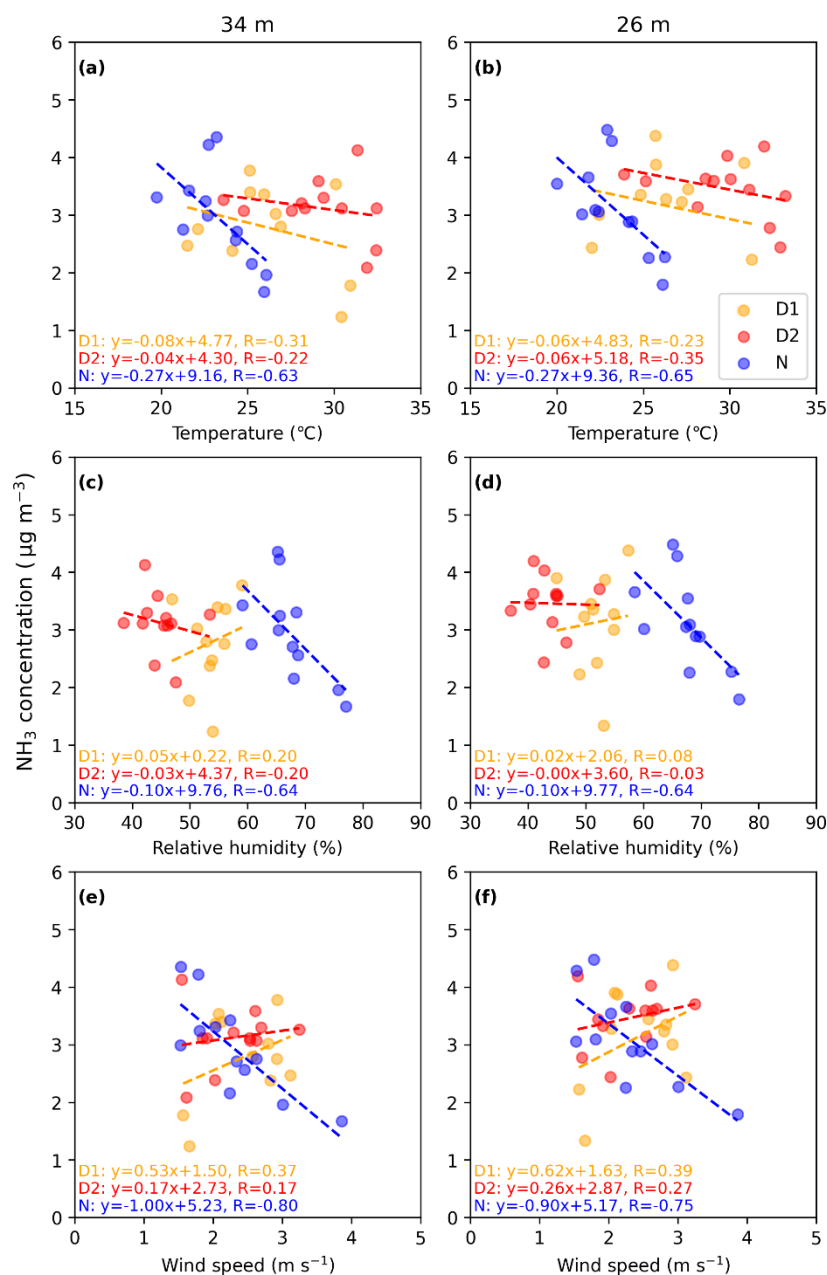


**Figure 6: Relationship between  $\text{NH}_3$  concentration at each height (34 m: (a), (c), (e); 26 m: (b), (d), (f)) and air temperature, relative humidity, and wind speed during the second half. Air temperature and relative humidity were recorded at 34 m ((a), (c)) and 26 m ((b), (d)), and wind speed only recorded at 31.5 m of the observation tower.**

The distribution of  $\text{NH}_3$  concentration relative to the main wind direction at each sampling time is shown in Fig. 7. Because the eastern side of the SERS is mainly covered by agricultural fields and residential areas (Fig. 1), there were concerns about





the potential influence of anthropogenic sources on the variation in  $\text{NH}_3$  concentration. Although the number of samples with wind directions other than east was limited, there was no noticeable difference in concentration levels compared to samples with an easterly wind. It is likely that there was little influence from anthropogenic sources because  $\text{NH}_3$  concentrations were not particularly high when the main wind direction was from the east, regardless of the observation period. Moreover, the fact that  $\text{NH}_3$  concentrations at 26 m were often higher than those at 34 m further supports the idea that variations in  $\text{NH}_3$  concentrations were not influenced by the presence of agricultural fields or residential areas.

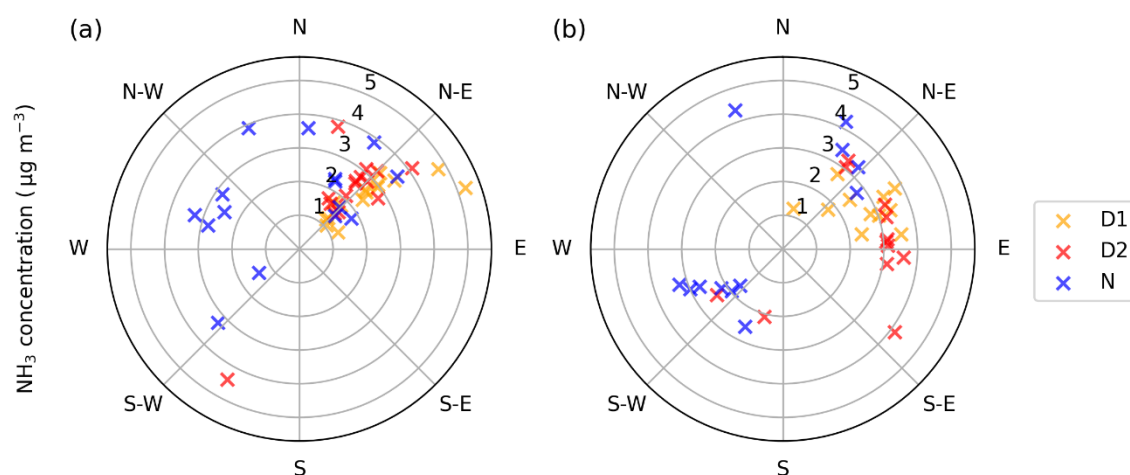


**Figure 7: The distribution of  $\text{NH}_3$  concentration at 34 m relative to the main wind direction at each sampling time during the first half (a) and second half (b) of the observation period.**

### 3.3 Ammonia fluxes and sources in the tropical dry deciduous forest

Prior to flux determination, we examined the diurnal variation in transfer velocity and its relationship with meteorological factors (Fig. 8). Focusing on diurnal variations, the transfer velocity tended to increase from 8:00, peak around noon, and then decrease after 17:00, regardless of the observation period. Our daytime sampling fell within this time window and successfully captured large daytime turbulence. Although the transfer velocity at nighttime was notably lower than that during the daytime, it remained above a certain level. The transfer velocity increased curvilinearly with increasing kinematic heat flux and friction velocity, regardless of the observation period. The kinematic heat flux tended to be larger in the second half of the observation period, whereas the level of friction velocity was almost the same, suggesting that the difference in the magnitude of the transfer velocity between each observation period was due to the difference in the kinematic heat flux, which is a parameter characterizing the turbulent transport of heat.

For flux determination, it is crucial to obtain accurate  $\Delta C$  because it determines the direction and magnitude of fluxes, while transfer velocity only determines the magnitude. In addition, the transfer velocity was calculated using meteorological



elements with roughly patterned diurnal and seasonal variations. On the other hand,  $\Delta C$  is calculated from the concentrations that are determined at multiple heights by multiple processes (i.g. installation of air sampler, collection of the sample, pre-processing for analysis, analysis using ion chromatograph). The diurnal and seasonal variations in concentrations are greatly influenced by the presence of emission sources as well as meteorological elements. Therefore, we performed a paired t-test on the obtained concentrations at 34 m and 26 m for quality assurance of  $\Delta C$  in addition to analysis by two ion chromatographs. As a result,  $\Delta C$  was significant ( $p < 0.01$ ) regardless of the observation period.  $\Delta C$  was also significant for two daytime ( $p < 0.01$ ) and nighttime ( $p < 0.05$ ) samples.

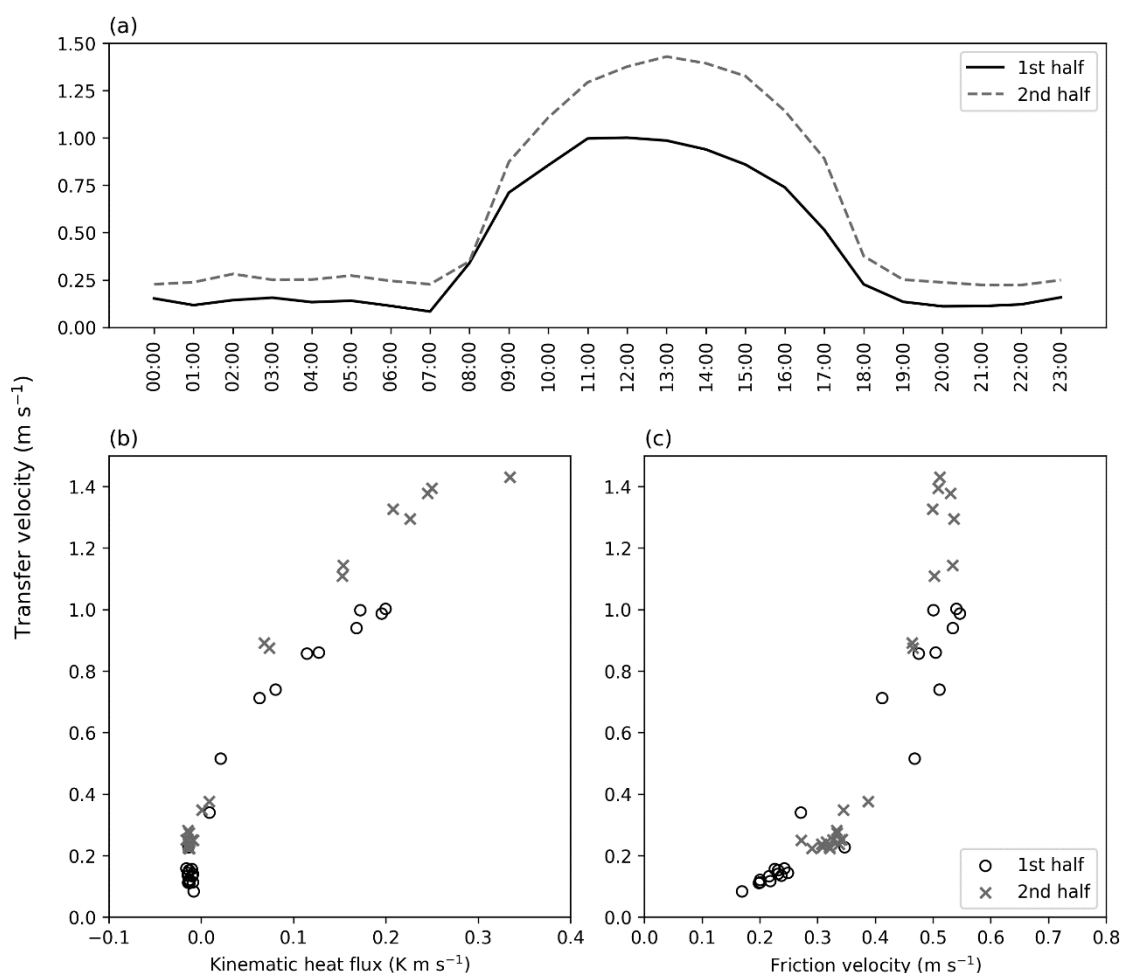
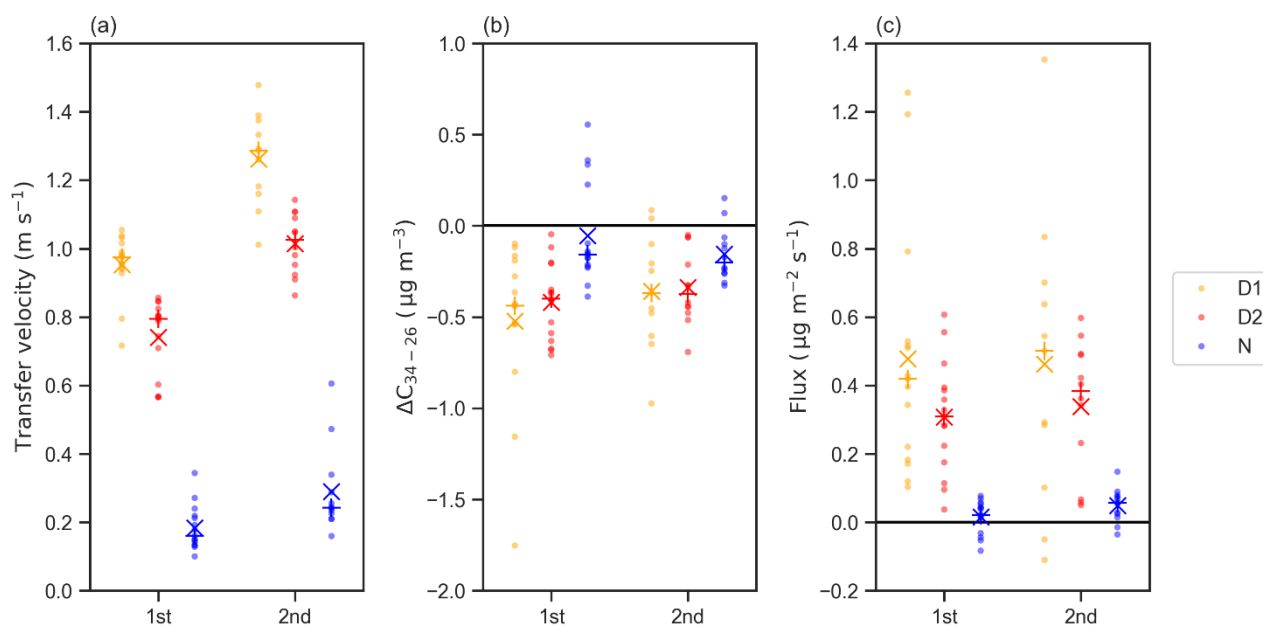


**Figure 8: Diurnal variation in the transfer velocity (a) and the relationship between transfer velocity with kinematic heat flux (b) and friction velocity (c) during the first half (solid line and circles) and second half (dashed line and crosses) of the observation period. The 1-h ensemble mean values for each observation period are shown.**



Fig. 9 shows the distribution of transfer velocity,  $\Delta C$ , and  $\text{NH}_3$  flux at each sampling time during the first and second halves of the observation period. The mean and median values for each item during the daytime and nighttime were almost the same. Transfer velocity was in the range from 0.10 to 1.48  $\text{m s}^{-1}$ , and tended to be higher during the daytime and in the second half of the observation period. The weighted means and standard deviations of transfer velocity by sampling time were  $0.40 \pm 0.33 \text{ m s}^{-1}$  and  $0.56 \pm 0.41 \text{ m s}^{-1}$  during the first and second halves, respectively. The weighted mean value of the transfer velocity between D1 and N differed by about four times.  $\Delta C$  was in the range from  $-1.75$  to  $0.56 \mu\text{g m}^{-3}$ , and there was little difference between observation periods except for some variations during the first half. The weighted means and standard deviations of  $\Delta C$  by sampling time were  $-0.19 \pm 0.35 \mu\text{g m}^{-3}$  and  $-0.21 \pm 0.20 \mu\text{g m}^{-3}$  during the first and second halves, respectively. Although the difference was not notable compared to transfer velocity, the absolute values of mean and median  $\Delta C$  at daytime were larger than those at nighttime. Flux was in the range from  $-0.110$  to  $1.352 \mu\text{g m}^{-2} \text{ s}^{-1}$ , and the absolute values had a clear trend to be larger at daytime reflecting the characteristics of transfer velocity and  $\Delta C$ . However, no clear difference was observed between the two periods as the transfer velocity. The weighted means and standard deviations of flux by sampling time were  $0.140 \pm 0.240 \mu\text{g m}^{-2} \text{ s}^{-1}$  and  $0.158 \pm 0.239 \mu\text{g m}^{-2} \text{ s}^{-1}$  during the first and second halves, respectively. As described in Sect. 3.2, there were significant changes in some meteorological elements and canopy conditions between the first and second halves of the observation period. However, regardless of the observation period,  $\text{NH}_3$  showed consistent pattern of air-forest exchange, with large emissions at the daytime, and small emissions and depositions at nighttime. The weighted mean and standard deviation of  $\text{NH}_3$  flux for the entire observation period was  $0.148 \pm 0.240 \mu\text{g m}^{-2} \text{ s}^{-1}$ , indicating that the tropical DDF of SERS acted as an emission source of  $\text{NH}_3$  during the dry season.





310 **Figure 9: Distribution of transfer velocity (a), NH<sub>3</sub> concentration difference between 34 m and 26 m (b), and NH<sub>3</sub> flux (c) at each sampling time during the first and second halves of the observation period. Positive value of flux indicates emission and negative value indicate deposition. Crosses and pluses indicate the mean and median values for each sampling time.**

Compared to the fluxes shown in recent studies over forest sites, those obtained in this study fell within these ranges, but the mean values were the largest. NH<sub>3</sub> fluxes over a Brazilian Amazon forest measured by Ramsay et al. (2020) using AGM ranged from  $-30.2$  to  $9.5 \text{ ng m}^{-2} \text{ s}^{-1}$  with mean and standard deviation of  $2.83 \pm 0.94 \text{ ng m}^{-2} \text{ s}^{-1}$ . Xu et al. (2023) measured NH<sub>3</sub> fluxes using AGM over a Japanese deciduous forest, and fluxes ranged from  $-0.256$  to  $0.335 \text{ } \mu\text{g m}^{-2} \text{ s}^{-1}$  with mean and standard deviation of  $0.057 \pm 0.120 \text{ } \mu\text{g m}^{-2} \text{ s}^{-1}$  during summer. More recently, Melman et al. (2025) measured NH<sub>3</sub> flux also using AGM over a Dutch coniferous forest, and showed range from  $-1.9$  to  $1.4 \text{ } \mu\text{g m}^{-2} \text{ s}^{-1}$  with mean of  $-0.050 \text{ } \mu\text{g m}^{-2} \text{ s}^{-1}$ . However, it should be noted that the measurement devices, errors, seasons, times, NH<sub>3</sub> concentrations, meteorological conditions, and statistical methods used in these studies were substantially different, and a direct comparison is only a rough guide. Therefore, we investigated the characteristics of seasonal and diurnal variations in NH<sub>3</sub> fluxes. 1-month of hourly measurements by Ramsay et al. (2020) indicated NH<sub>3</sub> emissions were likely to occur in the afternoon (from 14:00 to 16:00). Xu et al. (2023) showed seasonal and diurnal differences in fluxes, with the largest emissions occurring during the summer and daytime (from 8:00 to 17:00). 2-year measurements by Melman et al. (2025) characterized seasonal and diurnal NH<sub>3</sub> exchange: emissions around noon in summer and deposition in spring, autumn, and winter. Although the time periods of NH<sub>3</sub> emissions varied in these studies, emissions consistently occurred during the daytime in the warm season. Therefore, it can be said that our results are plausible.

Same with previous studies, those mentioned above speculated that daytime NH<sub>3</sub> emissions were mainly derived from the stomata of plants. However, Ramsey et al. (2020) and Melman et al. (2025) did not measure stomatal conductance ( $g_s$ ), a parameter indicating the degree of stomatal opening or ease of gas flow. Husted and Schjoerring (1996) obtained a linear relationship between NH<sub>3</sub> flux and leaf conductance in oilseed rape (*Brassica napus*) under controlled environmental conditions. Gessler et al. (2000) also found that NH<sub>3</sub> fluxes depend linearly on water vapor conductance, which is also an index of stomatal opening, in mature beech trees (*Fagus sylvatica*) at a German field site using a dynamic chamber technique. In the deciduous forest site studied by Xu et al. (2023), Tanaka et al. (2023) estimated  $g_s$  for the dominant species around the observation tower (*Quercus serrata*).  $g_s$  in August 2020 peaked during 9:00 to 16:00, and there was no change during this time. The daytime observations of Xu et al. (2023) were conducted during this time and fluxes correlated strongly with solar radiation, which is also a meteorological element that strongly controls  $g_s$ . Pitman (1996) showed  $g_s$  for six species including a dominant species (*Hopea ferrea*) in a dry evergreen forest of SERS and found that the peaks of  $g_s$  typically occurred between 9:00 and 12:00. This also coincides with the sampling time of D1, when the largest emissions were observed. The differences in the timing of daytime NH<sub>3</sub> emissions in these studies may reflect the differences in  $g_s$ . Igarashi et al. (2015) measured  $g_s$  in teak (*Tectona grandis* Linn. f.) in a typical tropical deciduous forest located in northern Thailand over six years and found that  $g_s$  had a hysteretic relationship with the LAI. They also revealed that  $g_s$  tended to be largest when LAI is



between 2.5 and 3.0, and tended to be smaller as LAI decrease during the dry season. Because the mean LAI at the DDF of  
345 SERS at the beginning of the first half was approximately 3.1, it is likely that gas exchange between the leaf stomata and the  
atmosphere was most active during this period. However, as can be seen from the decrease in LAI (Fig. A3), it was difficult  
to consider that emissions were mainly from the stomata during the second half when leaf fall progressed. However, the  
fluxes in the second half were at the same level as those in the first half, and indicating there must have been an alternative  
source of emissions to the leaf stomata (Fig. 9).

350 Based on previous findings summarized by Flechard et al. (2013), soil and leaf litter were the most likely emission sources in  
the second half. Ueda et al. (2017) specified the soil in the DDF as Ultisols, which are usually acidic, poor nutrient, and have  
a low content of organic matter. According to Tammadid et al. (2024), the soil pH in the DDF of SERS was in the range  
from 4.44 to 4.73, with a mean value of 4.54 (acidic). Xu et al. (2024) analyzed soil (Andosols) at the same forest site as Xu  
et al. (2023) and Tanaka et al. (2023), and found that the possibility of emissions from acidic soil ( $\text{pH} = 5.4$ ) was extremely  
355 low. Moreover, no ammonium ions were detected in the soil in the measurements. The same is probably true for the soil in  
the DDF of SERS, which has an even lower pH and poorer nutrient. In addition to soil analysis, Tammadid et al. (2024)  
revealed the litterfall production was highest in January (about  $1.5 \text{ tons dry matter ha}^{-1}$ ) and lowest in December in the DDF  
of SERS. During this period, the LAI in the DDF usually decreases considerably and is accompanied by leaf fall (Matsuda et  
al., 2012). Hansen et al. (2013) measured  $\text{NH}_3$  flux using the relaxed eddy accumulation method (REA) over a deciduous  
360 forest in Denmark and found a shift in the direction of flux from deposition to emission, with a simultaneous decrease in LAI.  
Their analysis, using a bi-directional exchange model, also indicated that litter is one of the main sources of  $\text{NH}_3$  emissions.  
A vertical profile measurement using the denuder sampling technique by Xu et al. (2024) at the same forest site as that of Xu  
et al. (2023) also revealed large  $\text{NH}_3$  emissions from the forest floor immediately after leaf fall. LAI during the emission  
period decreased by about half from 2.5 to 1.3 in 1 month in Xu et al. (2024), which is very closed to the LAI change in the  
365 DDF of SERS. While previous studies suggest that emissions from the decomposition of leaf litter are likely to occur under  
humid conditions (Hansen et al., 2013), the leaching of inorganic compounds from leaf litter is a rather unique process under  
the highly dry conditions of forests in Thailand. For example, Yamashita et al. (2010) conducted vertical flux measurements  
of inorganic nitrogen using ion exchange resin and buried bag methods in a dry evergreen forest of SERS and found that  
leaching of inorganic nitrogen from the leaf litter into the soil was substantially larger than atmospheric nitrogen deposition  
370 and that leaf litter served as the primary source of ammonium in the forest. It is possible that a portion of the  $\text{NH}_3$  produced  
during leaf litter decomposition is emitted into the atmosphere as the dry season and leaf fall progressed. In Hansen et al.  
(2013), flux measurements were conducted under conditions where both air and soil temperatures were below  $10^\circ\text{C}$ , raising  
concerns regarding whether leaf litter decomposition could progress under these low-temperature conditions. In contrast, the  
air temperature at SERS was higher throughout the observation period, suggesting more favorable conditions for  
375 decomposition. This evidence supports the idea that the source of  $\text{NH}_3$  emissions in the DDF of the SERS shifted  
dynamically from stomata in the first half (December) to leaf litter in the second half (from January to February). As we only



performed flux measurements in this time, it is further emphasized that it is necessary to measure plant physiological parameters such as stomatal conductance, as well as leaf litter production and emission potential in the future.

### 3.4 Factors controlling ammonia fluxes

380 Unlike the  $\text{NH}_3$  concentration and transfer velocity, no clear correlation was found between the  $\text{NH}_3$  flux and the meteorological elements, regardless of the observation period. This is thought to be due to the large variability in the flux and/or the complexity of the flux determination. Therefore, we divided air temperature, relative humidity, friction velocity, and solar radiation into several categories according to their ranges and focused on the flux distribution in each category (Fig. 10). As shown in Fig. 10, the ranges of temperature and relative humidity were slightly different because there were  
385 differences in the variation between the first and second halves of the observation periods. Regardless of the observation period,  $\text{NH}_3$  fluxes clearly showed trends according to the ranges of these meteorological elements: larger emissions when the temperature and the friction velocity were higher and the integrated solar radiation was larger. And fluxes shifted toward deposition as the relative humidity increased.

Observations and bi-directional exchange models have demonstrated that temperature is the most important factor  
390 controlling  $\text{NH}_3$  emissions (Flechard et al., 2013; Zhang et al., 2010). However, to the best of our knowledge, only a few field studies have clearly demonstrated the relationship between flux and temperature in forest sites. While no direct correlation could be found in Xu et al (2023), emissions tended to occur when the air temperature near the canopy was larger than 27 °C. They also found emissions likely to occur under dry conditions; relative humidity below 70%. Several field studies have also pointed to humidity and surface wetness as factors controlling flux (Ramsay et al., 2021; Hansen., 2013).  
395 Neirynck et al. (2005) measured the  $\text{NH}_3$  flux over a mixed suburban forest in Belgium and suggested that a wetted canopy may be a more efficient sink than a dry canopy. Regardless of the observation period,  $\text{NH}_3$  emission changed obviously at a temperature of 25°C and relative humidity of 60%, which is consistent with previous findings. Although further verification is needed at other observation sites, it is possible that the tropical dry deciduous forest exists in environments where emissions are more likely to occur during the dry season. At the same forest site as Xu et al. (2023), observations using the  
400 REA method have shown that friction velocity strongly controls  $\text{HNO}_3$  emissions (Xu et al., 2021). This study confirmed large  $\text{NH}_3$  fluxes with increase in friction velocity, indicating that the emission was enhanced by turbulence. During both the first and second halves, emissions are likely to occur with increase in air temperature and integrated solar radiation. However, based on the previous discussion, the roles of temperature and solar radiation may have differed during these periods. During the first half, when leaves were still abundant, solar radiation contributed to the opening of leaf stomata, which might  
405 indirectly facilitate emissions from leaves with increasing temperature. On the other hand, in the second half when there were fewer or no leaves and leaf litter was abundant, the forest floor was warmed by direct sunlight. Warm condition probably promoted the decomposition of leaf litter, resulting in continuous  $\text{NH}_3$  emissions. In the first half, the median flux increased stepwise in response to the amount of integrated solar radiation. In contrast, the change in median flux after the





first increase was smaller in the second half. These results may also be due to the different roles of solar radiation during the observation periods.

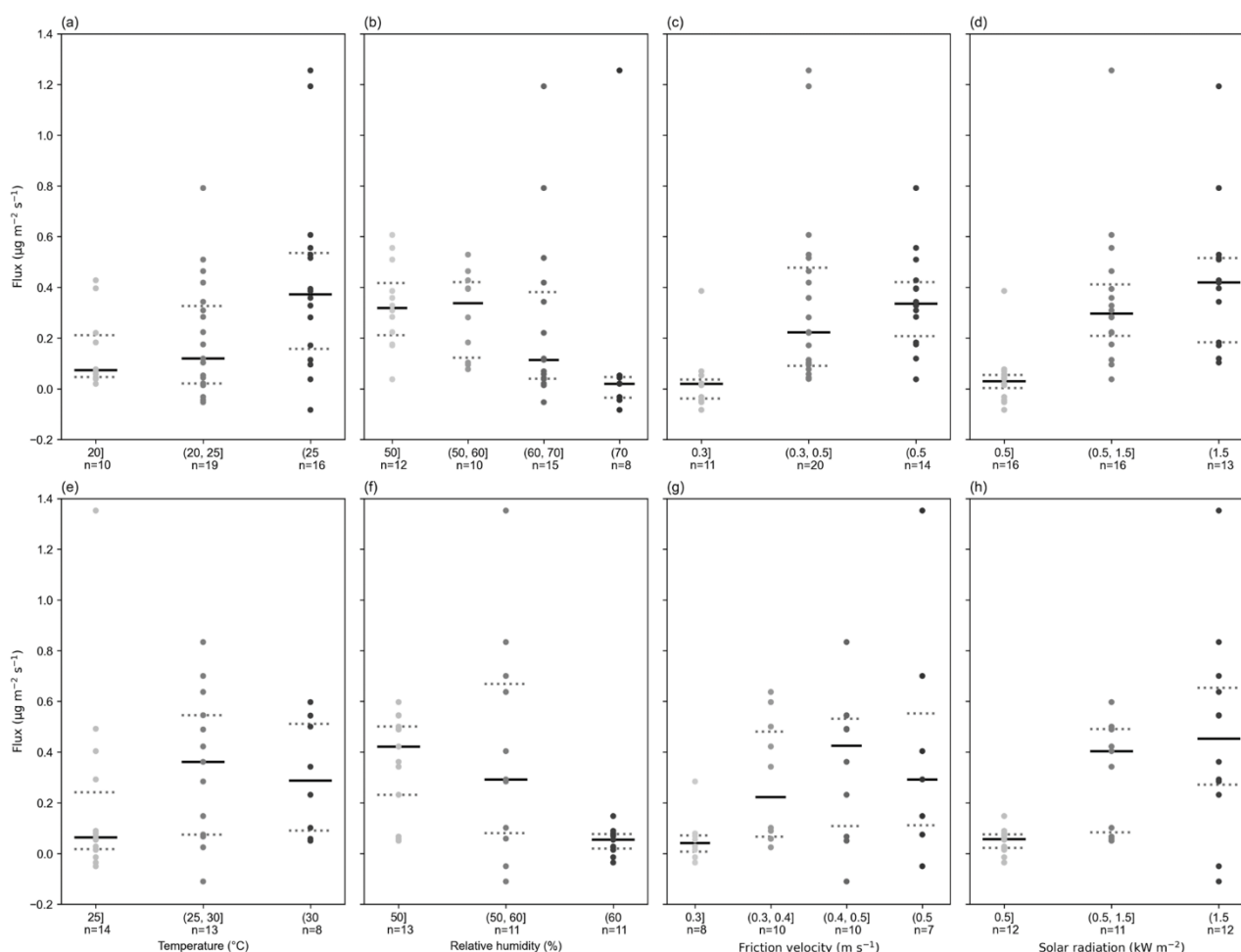


**Figure 10:** Distribution of  $\text{NH}_3$  flux according to the range of air temperature ((a), (e)), relative humidity ((b), (f)), friction velocity ((c), (g)), and solar radiation ((d), (h)) at each sampling time during the first half ((a), (b), (c), (d)) and second half ((e), (f), (g), (h)) of the observation period. Solid line indicates median value and dashed lines indicate the 75th (top) and 25th (bottom) percentiles. “(x)” indicates values greater than x, and “x]” indicates values less than or equal to x. Air temperature and relative humidity were recorded at 34 m, and friction velocity were derived at 31.5 m at the observation tower. Solar radiation was recorded at the weather station of SERS and the integrated values of 1-h values during each sampling time are shown.

### 3.5 Uncertainties

The AGM has larger measurement errors than more direct measurement methods, such as the REA and eddy covariance methods, because this method assumes steady-state conditions and derives flux from the difference in concentrations



measured at two heights. Although the case is limited, several high-time resolution flux observations using AGM over forests have shown levels of measurement error in  $\text{NH}_3$  fluxes. Wolff et al. (2010) obtained a median flux error of approximately 50% for a German spruce forest. A median error of 33 % was calculated for the study of Ramsay et al. (2020). Melman et al. (2025) reported a median random error of approximately 50%, indicating that the random error varies depending on season and sometime can be up to about 175%. The fluxes measured in this study are in the range of  $-0.110$  to  $1.352 \mu\text{g m}^{-2} \text{s}^{-1}$ , which probably includes some measurement errors. Manual measurements, such as those in this study, have limitations in term of time resolution for flux measurements and the number of samples that can be obtained during a campaign. Therefore, it is technically difficult to show measurement error statistically, as in previous studies. However, even if there was a measurement error of approximately 50% or more as reported in previous studies, the direction of the daytime  $\text{NH}_3$  flux tended to show upward throughout the observation period. Therefore, the conclusion that the tropical DDF acts as a net source of  $\text{NH}_3$  during the dry season remains robust.

In addition, the fluxes obtained in this study may have included outliers. Regardless of the observation period, all values that appeared to be outliers were obtained at sampling time of D1 (Fig. 9). This result cannot be easily interpreted as a coincidence. In agricultural fields, specific large emission events can be observed after fertilization, which are unthinkable at the forest site. Based on the findings published in recent years, the dynamic exchange mechanism at the canopy and/or ground surfaces could be a reasonable factor causing abnormally large  $\text{NH}_3$  emissions. According to Saylor et al. (2025), dew at surfaces may have a significant impact on  $\text{NH}_3$  bi-directional exchange; dew formation induces  $\text{NH}_3$  dissolution in moisture (absorption), and dew evaporation due to drying of the surface causes the re-emission of  $\text{NH}_3$  to the atmosphere. Field measurements across different surfaces have shown peaks in  $\text{NH}_3$  concentrations in the morning with a decrease in relative humidity, confirming this process (Wentworth et al., 2016). Although dew formation may seem unlikely in the DDF during the dry season, the meteorological conditions necessary for dew formation are frequently met during the nighttime. These include a sharp decrease in air temperature, lower wind speed, and an increase in relative humidity. Even in the absence of dew, the formation of a thin water film on the surfaces may play a similar role in the absorption and re-emission of  $\text{NH}_3$ . The nighttime fluxes on 16 December and 29 January were the few cases that showed deposition during the observation period; fluxes were  $-0.083 \mu\text{g m}^{-2} \text{s}^{-1}$  and  $-0.036 \mu\text{g m}^{-2} \text{s}^{-1}$ , respectively. Relative humidity at 34 m increased from the night of 16 December until 7:30 of 17 December and dropped from 87% to 63% until 12:40. Same variation was also observed from the night of 29 January to the noon of 30 January; relative humidity dropped from 82% to 46%. Temperature also increased up to about  $29^\circ\text{C}$  during both periods. The daytime fluxes (D1) on 17 December and 30 January showed large emissions; fluxes were  $1.256 \mu\text{g m}^{-2} \text{s}^{-1}$  and  $0.834 \mu\text{g m}^{-2} \text{s}^{-1}$ , respectively. This result led us to believe that the dynamic mechanism described above may indeed be real. On the other hand, there were samples like 26 January (D1) which showed a large emission of  $1.352 \mu\text{g m}^{-2} \text{s}^{-1}$  even though no deposition occurred at the night before. In addition to dew formation, changes in dew pH may affect bi-directional exchange because the equilibrium between gaseous-phase and liquid-phase  $\text{NH}_3$  also depends on pH. For example, acidic dew is thought to promote the deposition of  $\text{NH}_3$  and suppress the deposition of other acid gases (Wentworth et al., 2016). The pH of the dew on the surface is more complex and probably



depend on the amount and chemistry of the previously deposited substances. Because our observations alone cannot allow for further discussion about this mechanism, we should use bi-directional exchange models considering the dynamic exchange on surfaces (Sutton et al., 1998) to verify this hypothesis as the next step.

## 460 4 Conclusion

In this study, we conducted  $\text{NH}_3$  flux measurements in a tropical DDF in Thailand for the first time and found that the characteristics of  $\text{NH}_3$  concentration and flux were generally consistent with those of previous studies. On the other hand, we hypothesize that  $\text{NH}_3$  concentrations are controlled by meteorological elements as well as by changes in canopy structure accompanied by defoliation. Specifically, the dominant  $\text{NH}_3$  emission source may shift dynamically from leaf stomata to leaf  
465 litter in response to changes in canopy, forest floor, and meteorological conditions. Notably, during the observation period (December 2023 to February 2024), the monthly mean air temperatures were 1.2 to 1.8 °C higher than the monthly mean values over the 3-year from 2020 to 2022. In addition, the total annual rainfall in 2023 was 550 mm lower than the 3-year mean. These warmer and drier conditions may have suppressed  $\text{NH}_3$  deposition during the dry season. Observations under representative environmental conditions during both the dry and wet seasons are scheduled to be conducted in future studies.  
470 To draw a conclusion, measuring meteorological elements, concentrations, and fluxes alone is insufficient. Future studies must incorporate measurements of plant physiological parameters such as stomatal conductance, capturing surface wetness and dew formation, in addition to the analysis of leaf litter and soil parameters.

Improving the measurement accuracy using more advanced techniques is also a crucial next step, and we are currently addressing this challenge by installing an REA system (Xu et al., 2022; Xu et al., 2021) at the DDF of SERS. Moreover, high  
475 temporal resolution is an essential issue that must be addressed in future studies. Furthermore, the applicability of bi-directional exchange models in the tropical DDF is planned to be quantitatively evaluated as the next step, and model inter-comparison, as in Jongenelen et al. (2025), should also be conducted. Although some recent studies tend to rely heavily on sensitivity analyses of  $\text{NH}_3$  emission potentials of leaf stomata and soil and related resistances, it is scientifically more appropriate to improve and refine models based on onsite information and conditions. The  $\text{NH}_3$  bi-directional exchange  
480 processes and emission sources can be accurately characterized only through such integrative approaches. In recent years, there have been studies that treat the bi-directional exchange of  $\text{NH}_3$  in regional scale chemical transport models (Fu et al., 2015; Bash et al., 2013). A global scale estimate of  $\text{NH}_3$  deposition considering bi-directional exchange was also conducted using a satellite-based technique (Liu et al., 2020). Detailed assessments of atmospheric deposition processes have also been conducted from point models to regional models, such as in AQMEII4 project (Galmarini et al., 2021). This study presents a  
485 valuable dataset for verifying the results of these latest studies and contributes to the further improvement of the models.



## Appendix A: Additional figures

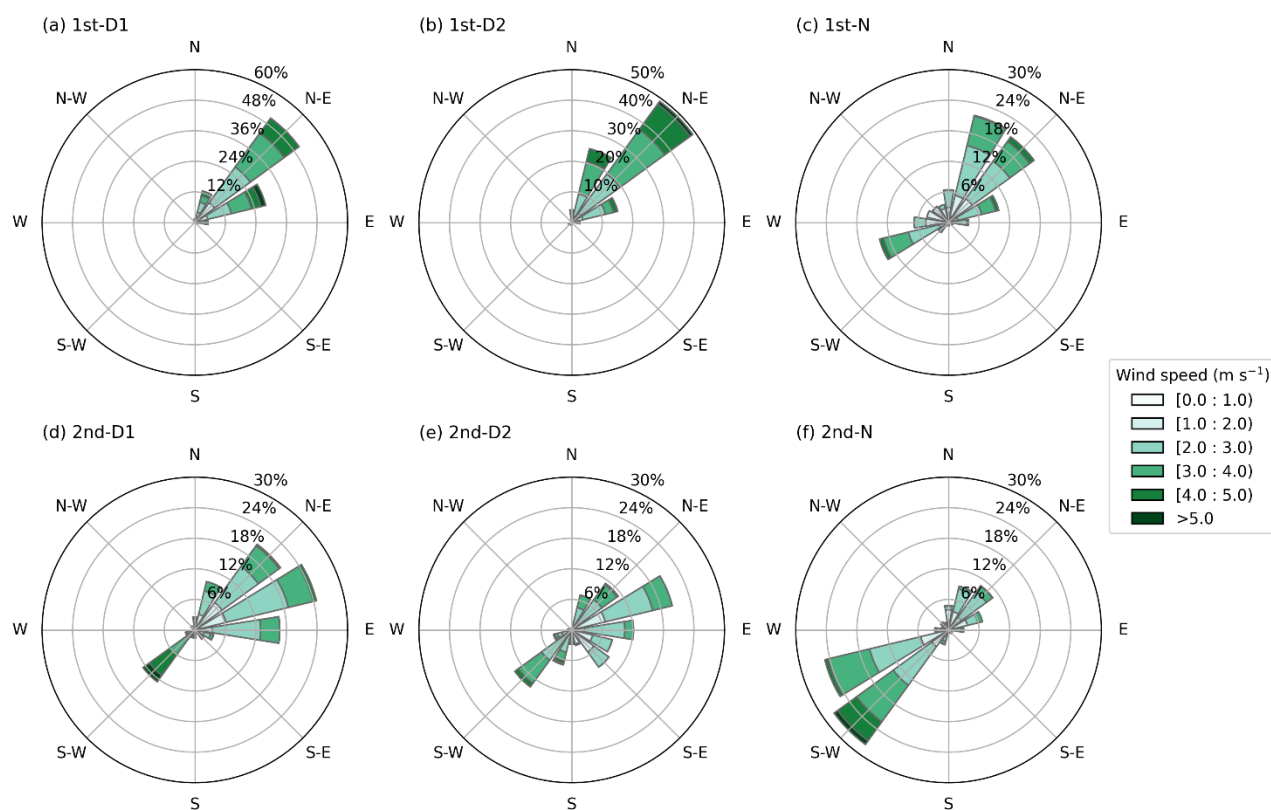
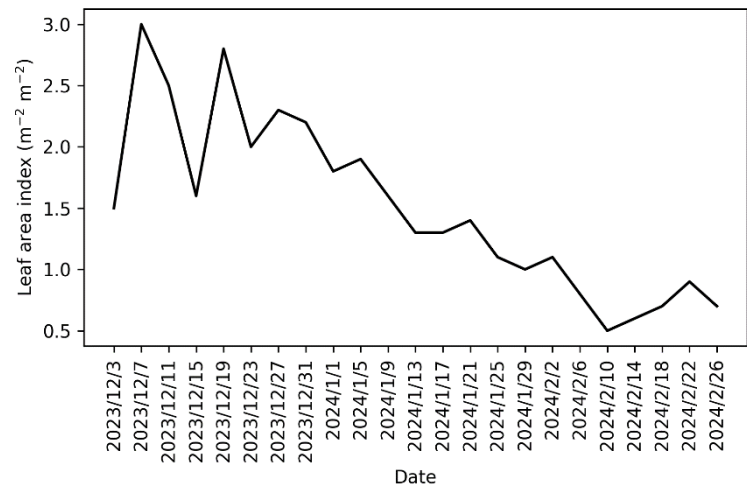


**Figure A1:** Windrose at sampling time of D1 ((a), (d)), D2 ((b), (e)), and N ((c), (f)) during the first half ((a), (b), (c)) and the second half ((d), (e), (f)) of the observation period.

490

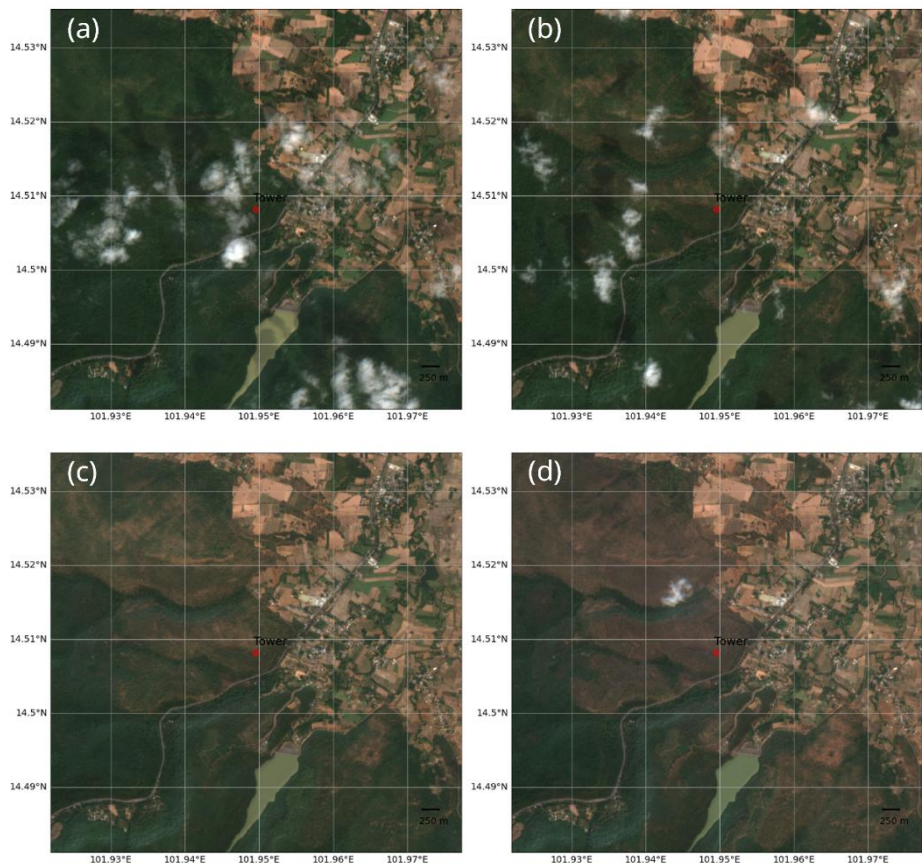


**Figure A2:** Canopy conditions of the dry deciduous forest around the observation tower at the begging of the first half (a) and second half (b), and the end of the campaign (c). All the photos were taken from the same direction facing north.



495

**Figure A3: Variation in the satellite-derived LAI at the observation tower. The dataset of MCD15A3H, which is the product of the Moderate Resolution Imaging Spectroradiometer mounted at the satellite Terra and Aqua was used.**







500 **Figure A4: Satellite imagery (6 km × 6 km) of the observation site during four periods: (a) December 15–31, 2023; (b) January 1–10, 2024; (c) January 11–21, 2024; and (d) January 22–February 7, 2024. The images were retrieved from the dataset of Sentinel-2 Surface Reflectance Harmonized (COPERNICUS/S2\_SR\_HARMONIZED) via © Google Earth Engine. For each period, imagery was filtered for the observation site, and scenes with cloud cover below 20% were selected.**

### Data availability

505 The dataset of flux measurements in this study are available from the corresponding author on reasonable request.

### Author contributions

MX: conceptualization, methodology, formal analysis, visualization, investigation, writing (original draft). PC: resources, investigation, writing (review and editing). HS: investigation, writing (review and editing). AS: writing (review and editing). SI: software, writing (review and editing). KM: conceptualization, investigation, supervision, project administration, funding  
510 acquisition.

### Competing interests

The authors declare that they have no conflict of interest.

### Acknowledgements

We gratefully acknowledge the support of Dr. Surachit Waengsothorn (Thailand Institute of Scientific and Technological  
515 Research), Ms. Kanoktip Somsiri (Thailand Institute of Scientific and Technological Research), and all members of the Sakaerat Environmental Research Station.

### Financial support

This work was supported by JSPS KAKENHI (Grant Numbers 23KK0190) and the project “Research on biodiversity and ecosystem conservation taking into account synergies and trade-offs of ecosystem services” (Prof. Shinsuke Koike’s team)  
520 of Institute of Global Innovation Research, Tokyo University of Agriculture and Technology.

### References

Ban, S., Matsuda, K., Sato, K., and Ohizumi, T.: Long-term assessment of nitrogen deposition at remote EANET sites in Japan, Atmos. Environ., 146, 70–78, <https://doi.org/10.1016/j.atmosenv.2016.04.015>, 2016.





- 525 Ban, S., Matsuda, K., and Ohizumi, T.: A method estimating dry deposition for assessment of nitrogen load on forests in  
East Asia, *Water Air Soil Pollut.*, 233, 417, <https://doi.org/10.1007/s11270-022-05874-5>, 2022.
- Bash, J. O., Cooter, E. J., Dennis, R. L., Walker, J. T., and Pleim, J. E.: Evaluation of a regional air-quality model with  
bidirectional NH<sub>3</sub> exchange coupled to an agroecosystem model, *Biogeosciences*, 10, 1635–1645,  
530 <https://doi.org/10.5194/bg-10-1635-2013>, 2013.
- Beachley, G. M., Fenn, M. E., Du, E., de Vries, W., Bauters, M., Bell, M. D., Kulshrestha, U. C., Schmitz, A., and Walker, J.  
T.: Monitoring nitrogen deposition in global forests, in: *Atmospheric Nitrogen Deposition to Global Forests*, edited by: Du,  
E. and de Vries, W., Elsevier, Amsterdam, Netherland, 17–38, <https://doi.org/10.1016/B978-0-323-91140-5.00019-1>, 2024.
- 535 Chanonmuang, P., Khummongkol, P., and Matsuda, K.: Dry deposition of SO<sub>2</sub> over dry dipterocarp forest, Thailand, *Sains  
Malays.*, 44(3), 317–323, <https://doi.org/10.17576/jsm-2015-4403-02>, 2015.
- Chatani, S., Shimadera, H., Kitayama, K., and Nishina, K.: Numerical analysis of factors causing long-term trends and  
540 annual variations of sulfur and nitrogen deposition amount in Japan from 2000 to 2020, *Asian J. Atmos. Environ.*, 19, 2,  
<https://doi.org/10.1007/s44273-025-00052-5>, 2025.
- Chen, S., Chen, B., Wang, S., Sun, L., Shi, H., Liu, Z., Wang, Q., Li, H., Zhu, T., Li, D., Xia, Y., Zhao, Z., Wang, L., and  
Wang, L.: Spatiotemporal variations of atmospheric nitrogen deposition in China during 2008–2020, *Atmos. Environ.*, 315,  
545 120120, <https://doi.org/10.1016/j.atmosenv.2023.120120>, 2023.
- EANET: Data Report 2023, available at: <https://monitoring.eanet.asia/document/public/download?cd=299>, last access: 19  
May 2025.
- 550 EANET: Data Report 2020, available at: <https://monitoring.eanet.asia/document/public/download?cd=262>, last access: 19  
May 2025.
- Endo, T., Yagoh, H., Sato, K., Matsuda, K., Hayashi, K., Noguchi, I., and Sawada, K.: Regional characteristics of dry  
deposition of sulfur and nitrogen compounds at EANET sites in Japan from 2003 to 2008, *Atmos. Environ.*, 45, 1259–1267,  
555 <https://doi.org/10.1016/j.atmosenv.2010.12.003>, 2011.



EPA: Reactive Nitrogen in the United States: An Analysis of Inputs, Flows, Consequences, and Management Options: A Report of the EPA Science Advisory Board, available at: <https://nepis.epa.gov/Exe/ZyPDF.cgi/P100DD0K.PDF?Dockey=P100DD0K.PDF>, last access: 19 May 2025.

560

Flechard, C. R., Massad, R.-S., Loubet, B., Personne, E., Simpson, D., Bash, J. O., Cooter, E. J., Nemitz, E., and Sutton, M. A.: Advances in understanding, models and parameterizations of biosphere-atmosphere ammonia exchange, *Biogeosciences*, 10, 5183–5225, <https://doi.org/10.5194/bg-10-5183-2013>, 2013.

565 Fu, X., Wang, S. X., Ran, L. M., Pleim, J. E., Cooter, E., Bash, J. O., Benson, V., and Hao, J. M.: Estimating NH<sub>3</sub> emissions from agricultural fertilizer application in China using the bi-directional CMAQ model coupled to an agro-ecosystem model, *Atmos. Chem. Phys.*, 15, 6637–6649, <https://doi.org/10.5194/acp-15-6637-2015>, 2015.

Galmarini, S., Makar, P., Clifton, O. E., Hogrefe, C., Bash, J. O., Bellasio, R., Bianconi, R., Bieser, J., Butler, T., Ducker, J., 570 Flemming, J., Hodzic, A., Holmes, C. D., Kioutsioukis, I., Kranenburg, R., Lupascu, A., Perez-Camanyo, J. L., Pleim, J., Ryu, Y.-H., San Jose, R., Schwede, D., Silva, S., and Wolke, R.: Technical note: AQMEII4 Activity 1: evaluation of wet and dry deposition schemes as an integral part of regional-scale air quality models, *Atmos. Chem. Phys.*, 21, 15663–15697, <https://doi.org/10.5194/acp-21-15663-2021>, 2021.

575 Gessler, A., Rienks, M., and Rennenberg, H.: NH<sub>3</sub> and NO<sub>2</sub> fluxes between beech trees and the atmosphere – correlation with climatic and physiological parameters, *New Phytol.*, 147(3), 539–560, <https://doi.org/10.1046/j.1469-8137.2000.00712.x>, 2000.

Hansen, K., Sørensen, L. L., Hertel, O., Geels, C., Skjøth, C. A., Jensen, B., and Boegh, E.: Ammonia emissions from 580 deciduous forest after leaf fall, *Biogeosciences*, 10, 4577–4589, <https://doi.org/10.5194/bg-10-4577-2013>, 2013.

Hayashi, K., Matsuda, K., Takahashi, A., and Nakaya, K.: Atmosphere–forest exchange of ammoniacal nitrogen in a subalpine deciduous forest in central Japan during a summer week, *Asian J. Atmos. Environ.*, 5, 134–143, <https://doi.org/10.5572/ajae.2011.5.2.134>, 2011.

585

Hayashi, K., Ono, K., Tokida, T., Takimoto, T., Mano, M., Miyata, A., and Matsuda, K.: Atmosphere–rice paddy exchanges of inorganic particles and relevant gases during a week in winter and a week in summer, *J. Agric. Meteorol.*, 68(1), 55–68, <https://doi.org/10.2480/agrmet.68.1.8>, 2012.



590 Hayashi, K., Ono, K., Matsuda, K., Tokida, T., and Hasegawa, T.: Characteristics of atmosphere–rice paddy exchange of gaseous and particulate reactive nitrogen in terms of nitrogen input to a single-cropping rice paddy area in central Japan, *Asian J. Atmos. Environ.*, 11, 202–216, <https://doi.org/10.5572/ajae.2017.11.3.202>, 2017.

Hayashi, K., Shibata, H., Oita, A., Nishina, K., Ito, A., Katagiri, K., Shindo, J., and Winiwarter, W.: Nitrogen budgets in Japan from 2000 to 2015: Decreasing trend of nitrogen loss to the environment and the challenge to further reduce nitrogen  
595 waste, *Environ. Pollut.*, 286, 117559, <https://doi.org/10.1016/j.envpol.2021.117559>, 2021.

Husted, S., and Schjoerring, J. K.: Ammonia flux between oilseed rape plants and the atmosphere in response to changes in leaf temperature, light intensity, and air humidity (interactions with leaf conductance and apoplastic  $\text{NH}_4^+$  and  $\text{H}^+$   
600 concentrations), *Plant Physiol.*, 112(1), 67–74, <https://doi.org/10.1104/pp.112.1.67>, 1996.

Igarashi, Y., Kumagai, T., Yoshifuji, N., Sato, T., Tanaka, N., Tanaka, K., Suzuki, M., and Tantasirin, C.: Environmental control of canopy stomatal conductance in a tropical deciduous forest in northern Thailand, *Agr. For. Meteorol.*, 202, 1–10, <https://doi.org/10.1016/j.agrformet.2014.11.013>, 2015.

605 Ishida, A., Yamaji, K., Nakano, T., Ladpala, P., Popradit, A., Yoshimura, K., Saiki, S., Maeda, T., Yoshimura, J., Koyama, K., Diloksumpun, S., and Marod, D.: Comparative physiology of canopy tree leaves in evergreen and deciduous forests in lowland Thailand, *Sci. Data*, 10, 601, <https://doi.org/10.1038/s41597-023-02468-6>, 2023.

610 Jongenelen, T., van Zanten, M., Dammers, E., Wichink Kruit, R., Hensen, A., Geers, L., and Erisman, J. W.: Validation and uncertainty quantification of three state-of-the-art ammonia surface exchange schemes using  $\text{NH}_3$  flux measurements in a dune ecosystem, *Atmos. Chem. Phys.*, 25, 4943–4963, <https://doi.org/10.5194/acp-25-4943-2025>, 2025.

Khoomsab, K., Khummongkol, P., and Matsuda, K.: Trends in sulfate dry deposition over mixed dipterocarp forest in  
615 Thailand using relaxed eddy accumulation method, *Sains Malaysiana*, 43(3), 369–375, 2014.

Kuriyama, K. and Hayashi, K.: Sustainable agriculture and the nitrogen issue, in: *Economics of Sustainable Agriculture*, edited by: Kuriyama, K., Global Environmental Studies, Springer, Singapore, [https://doi.org/10.1007/978-981-96-3502-3\\_1](https://doi.org/10.1007/978-981-96-3502-3_1), 2025.

620 Liu, L., Zhang, X., Xu, W., Liu, X., Wei, J., Wang, Z., and Yang, Y.: Global estimates of dry ammonia deposition inferred from space measurements, *Sci. Total Environ.*, 730, 139189, <https://doi.org/10.1016/j.scitotenv.2020.139189>, 2020.



- Matsuda, K., Watanabe, I., Wingpud, V., Theramongkol, P., Khummongkol, P., Wangwongwatana, S., and Totsuka, T.:  
625 Ozone dry deposition above a tropical forest in the dry season in northern Thailand, *Atmos. Environ.*, 39(14), 2571–2577,  
<https://doi.org/10.1016/j.atmosenv.2005.01.011>, 2005.
- Matsuda, K., Watanabe, I., Wingpud, V., Theramongkol, P., and Ohizumi, T.: Deposition velocity of O<sub>3</sub> and SO<sub>2</sub> in the dry  
and wet season above a tropical forest in northern Thailand, *Atmos. Environ.*, 40(39), 7557–7564,  
630 <https://doi.org/10.1016/j.atmosenv.2006.07.003>, 2006.
- Matsuda, K., Sase, H., Murao, N., Fukazawa, T., Khoomsub, K., Chanonmuang, P., Visaratana, T., and Khummongkol, P.:  
Dry and wet deposition of elemental carbon on a tropical forest in Thailand, *Atmos. Environ.*, 54, 282–287,  
<https://doi.org/10.1016/j.atmosenv.2012.02.022>, 2012.
- 635 Melman, E. A., Rutledge-Jonker, S., Frumau, K. F. A., Hensen, A., van Pul, W. A. J., Stolk, A. P., Wichink Kruit, R. J., and  
van Zanten, M. C.: Measurements and model results of a two-year dataset of ammonia exchange over a coniferous forest in  
the Netherlands, *Atmos. Environ.*, 344, 120976, <https://doi.org/10.1016/j.atmosenv.2024.120976>, 2025.
- 640 Murata, N., Ohta, S., Ishida, A., Kanzaki, M., Wachirinrat, C., Artchawakom, T., and Sase, H.: Comparison of soil depths  
between evergreen and deciduous forests as a determinant of their distribution, Northeast Thailand, *J. For. Res.*, 14(4), 212–  
220, <https://doi.org/10.1007/s10310-009-0127-7>, 2009.
- Murata, N., Ohta, S., Ishida, A., Kanzaki, M., Wachirinrat, C., Artchawakom, T., and Sase, H.: Soil depth and soil water  
645 regime in a catchment where tropical dry evergreen and deciduous forests coexist, *J. For. Res.*, 17(1), 37–44,  
<https://doi.org/10.1007/s10310-010-0248-z>, 2011.
- Myneni, R., Knyazikhin, Y., and Park, T.: MCD15A3H MODIS/Terra+Aqua Leaf Area Index/FPAR 4-day L4 Global 500 m  
SIN Grid V006, NASA EOSDIS Land Processes DAAC, <https://doi.org/10.5067/MODIS/MCD15A3H.006>, 2015.
- 650 Nakahara, S., Takagi, K., Sorimachi, A., Katata, G., and Matsuda, K.: Enhancement of dry deposition of PM<sub>2.5</sub> nitrate in a  
cool temperate forest, *Atmos. Environ.*, 212, 136–141, <https://doi.org/10.1016/j.atmosenv.2019.05.053>, 2019.
- Neiryneck, J., Kowalski, A. S., Carrara, A., and Ceulemans, R.: Driving forces for ammonia fluxes over mixed forest  
655 subjected to high deposition loads, *Atmos. Environ.*, 39(28), 5013–5024, <https://doi.org/10.1016/j.atmosenv.2005.05.027>,  
2005.



Nishina, K., Watanabe, M., Koshikawa, M. K., Takamatsu, T., Morino, Y., Nagashima, T., Soma, K., and Hayashi, S.: Varying sensitivity of mountainous streamwater base-flow  $\text{NO}_3^-$  concentrations to N deposition in the northern suburbs of Tokyo, Sci. Rep., 7, 7701, <https://doi.org/10.1038/s41598-017-07883-4>, 2017.

Nishina, K., Ito, A., Zhou, F., Yan, X., Hayashi, S., and Winiwarter, W.: Historical trends of riverine nitrogen loading from land to the East China Sea: a model-based evaluation, Environ. Res. Commun., 3(8), 085005, <https://doi.org/10.1088/2515-7620/ac1ce8>, 2021.

Nishina, K., Hayashi, K., Oita, A., Asada, K., Hayakawa, A., Okadera, T., Onodera, T., Hanaoka, T., Tsuchiya, K., Kobayashi, K., and Koga, N.: Feasibility assessment of Japan's fertilizer reduction target: A meta-analysis and its implications for nitrogen waste, J. Environ. Manage., 373, 123362, <https://doi.org/10.1016/j.jenvman.2024.123362>, 2025.

Osada, K.: Measurement report: Short-term variation in ammonia concentrations in an urban area increased by mist evaporation and emissions from a forest canopy with bird droppings, Atmos. Chem. Phys., 20, 11941–11954, <https://doi.org/10.5194/acp-20-11941-2020>, 2020.

Pitman, J. I.: Ecophysiology of tropical dry evergreen forest, Thailand: Measured and modelled stomatal conductance of *Hopea ferrea*, a dominant canopy emergent, J. Appl. Ecol., 33(6), 1366–1378, <https://doi.org/10.2307/2404777>, 1996.

Ramsay, R., Di Marco, C. F., Sörgel, M., Heal, M. R., Carbone, S., Artaxo, P., de Araújo, A. C., Sá, M., Pöhlker, C., Lavric, J., Andreae, M. O., and Nemitz, E.: Concentrations and biosphere–atmosphere fluxes of inorganic trace gases and associated ionic aerosol counterparts over the Amazon rainforest, Atmos. Chem. Phys., 20, 15551–15584, <https://doi.org/10.5194/acp-20-15551-2020>, 2020.

Ramsay, R., Di Marco, C. F., Heal, M. R., Sörgel, M., Artaxo, P., Andreae, M. O., and Nemitz, E.: Measurement and modelling of the dynamics of  $\text{NH}_3$  surface–atmosphere exchange over the Amazonian rainforest, Biogeosciences, 18, 2809–2825, <https://doi.org/10.5194/bg-18-2809-2021>, 2021.

Rubin, H. J., Fu, J. S., Dentener, F., Li, R., Huang, K., and Fu, H.: Global nitrogen and sulfur deposition mapping using a measurement–model fusion approach, Atmos. Chem. Phys., 23, 7091–7102, <https://doi.org/10.5194/acp-23-7091-2023>, 2023.

Rudek, J., Aneja, V. P., and Abrol, Y. P.: Concepts for considerations in the design of an Indian integrated nitrogen assessment, in: The Indian Nitrogen Assessment, edited by: Abrol, Y. P., Adhya, T. K., Aneja, V. P., Raghuram, N., Pathak,



- H., Kulshrestha, U., Sharma, C., and Singh, B., Elsevier, Amsterdam, 29–43, <https://doi.org/10.1016/B978-0-12-811836-8.00003-3>, 2017.
- Sase, H., Matsuda, K., Visaratana, T., Garivait, H., Yamashita, N., Kietvuttinon, B., Hongthong, B., Luangjame, J.,  
695 Khummongkol, P., Shindo, J., Endo, T., Sato, K., Uchiyama, S., Miyazawa, M., Nakata, M., and Lenggoro, I. W.:  
Deposition process of sulfate and elemental carbon in Japanese and Thai forests, *Asian J. Atmos. Environ.*, 6, 246–258,  
<https://doi.org/10.5572/ajae.2012.6.4.246>, 2012.
- Sase, H., Yamashita, N., Luangjame, J., Garivait, H., Kietvuttinon, B., Visaratana, T., Kamisako, M., Kobayashi, R., Ohta,  
700 S., Shindo, J., Hayashi, K., Toda, H., and Matsuda, K.: Alkalinization and acidification of stream water with changes in  
atmospheric deposition in a tropical dry evergreen forest of northeastern Thailand, *Hydrol. Process.*, 31(4), 836–846,  
<https://doi.org/10.1002/hyp.11062>, 2017.
- Saylor, R. D., Walker, J. T., Wu, Z., Chen, X., Schwede, D. B., Oishi, A. C., and Lichiheb, N.: Dynamic ammonia exchange  
705 within a mixed deciduous forest canopy in the Southern Appalachians, *Ecol. Model.*, 501, 111007,  
<https://doi.org/10.1016/j.ecolmodel.2024.111007>, 2025.
- Sutton, M. A., Howard, C. M., Erisman, J. W., Billen, G., Bleeker, A., Grennfelt, P., van Grinsven, H., and Grizzetti, B.  
(Eds.): *The European nitrogen assessment – sources, effects and policy perspectives*, Cambridge Univ. Press, Cambridge,  
710 <https://doi.org/10.1017/CBO9780511976988>, 2011.
- Sutton, M. A., Burkhard, J.K., Guerin, D., Nemitz, E., Fowler, D.: Development of resistance models to describe  
measurements of bi-directional ammonia surface–atmosphere exchange, *Atmos. Environ.*, 32(3), 473–480,  
[https://doi.org/10.1016/S1352-2310\(97\)00164-7](https://doi.org/10.1016/S1352-2310(97)00164-7), 1998.  
715
- Tammadid, W., Sangkachai, B., Chanonmuang, P., Chidthaisong, A., and Hanpattanakit, P.: Comparison and environmental  
controls of soil respiration in primary and secondary dry dipterocarp forests in Thailand, *Front. For. Glob. Change*, 7,  
1294942, <https://doi.org/10.3389/ffgc.2024.1294942>, 2024.
- 720 Tanaka, R., Chiu, C.-W., Gomi, T., Matsuda, K., Izuta, T., and Watanabe, M.: Stomatal ozone uptake of a *Quercus serrata*  
stand based on sap flow measurements with calibrated thermal dissipation sensors, *Sci. Total Environ.*, 888, 164005,  
<https://doi.org/10.1016/j.scitotenv.2023.164005>, 2023.





- Ueda, M. U., Kachina, P., Marod, D., Nakashizuka, T., and Kurokawa, H.: Soil properties and gross nitrogen dynamics in  
725 old growth and secondary forest in four types of tropical forest in Thailand, *For. Ecol. Manage.*, 398, 130–139,  
<https://doi.org/10.1016/j.foreco.2017.05.010>, 2017.
- Walker, J. T., Chen, X., Wu, Z., Schwede, D., Daly, R., Djurkovic, A., Oishi, A. C., Edgerton, E., Bash, J., Knoepp, J.,  
Puchalski, M., Iiames, J., and Miniati, C. F.: Atmospheric deposition of reactive nitrogen to a deciduous forest in the southern  
730 Appalachian Mountains, *Biogeosciences*, 20, 971–995, <https://doi.org/10.5194/bg-20-971-2023>, 2023.
- Wang, K., Kang, P., Lu, Y., Zheng, X., Liu, M., Lin, T.-J., Butterbach-Bahl, K., and Wang, Y.: An open-path ammonia  
analyzer for eddy covariance flux measurement, *Agric. For. Meteorol.*, 308–309, 108570,  
<https://doi.org/10.1016/j.agrformet.2021.108570>, 2021.  
735
- Wen, Z., Xu, W., Li, Q., Han, M., Tang, A., Zhang, Y., Luo, X., Shen, J., Wang, W., Li, K., Pan, Y., Zhang, L., Li, W.,  
Collett, J. L., Zhong, B., Wang, X., Goulding, K. W. T., Zhang, F., and Liu, X.: Changes of nitrogen deposition in China  
from 1980 to 2018, *Environ. Int.*, 144, 106022, <https://doi.org/10.1016/j.envint.2020.106022>, 2020.
- 740 Wentworth, G. R., Murphy, J. G., Benedict, K. B., Bangs, E. J., and Collett Jr., J. L.: The role of dew as a night-time  
reservoir and morning source for atmospheric ammonia, *Atmos. Chem. Phys.*, 16, 7435–7449, <https://doi.org/10.5194/acp-16-7435-2016>, 2016.
- Wolff, V., Trebs, I., Ammann, C., and Meixner, F. X.: Aerodynamic gradient measurements of the NH<sub>3</sub>-HNO<sub>3</sub>-NH<sub>4</sub>NO<sub>3</sub>  
745 triad using a wet chemical instrument: an analysis of precision requirements and flux errors, *Atmos. Meas. Tech.*, 3, 187–208,  
<https://doi.org/10.5194/amt-3-187-2010>, 2010.
- Wu, Z., Xu, M., Sorimachi, A., Sase, H., Watanabe, M., and Matsuda, K.: Dry deposition of nitric acid gas by long-term  
measurement above and below a forest canopy, *Asian J. Atmos. Environ.*, 18, 11, [https://doi.org/10.1007/s44273-024-00034-](https://doi.org/10.1007/s44273-024-00034-z)  
750 [z](https://doi.org/10.1007/s44273-024-00034-z), 2024.
- Xu, M. and Matsuda, K.: Dry deposition of PM<sub>2.5</sub> nitrate in a forest according to vertical profile measurements, *Asian J.*  
*Atmos. Environ.*, 14, 367–377, <https://doi.org/10.5572/ajae.2020.14.4.367>, 2020.
- 755 Xu, M., Kasahara, K., Sorimachi, A., and Matsuda, K.: Nitric acid dry deposition associated with equilibrium shift of  
ammonium nitrate above a forest by long-term measurement using relaxed eddy accumulation, *Atmos. Environ.*, 256,  
118454, <https://doi.org/10.1016/j.atmosenv.2021.118454>, 2021.



- Xu, M., Umehara, M., Sase, H., and Matsuda, K.: Ammonia fluxes over an agricultural field in growing and fallow periods using relaxed eddy accumulation, *Atmos. Environ.*, 284, 119195, <https://doi.org/10.1016/j.atmosenv.2022.119195>, 2022.
- Xu, M., Chanonmuang, P., and Matsuda, K.: Vertical profile and flux measurements of ammonia in a deciduous forest in Japan towards improvement of bi-directional exchange model, *Atmos. Environ.*, 315, 120144, <https://doi.org/10.1016/j.atmosenv.2023.120144>, 2023.
- Xu, M., Matsumoto, R., Chanonmuang, P., and Matsuda, K.: Vertical profile measurements for ammonia in a Japanese deciduous forest using denuder sampling technique: ammonia emissions near the forest floor, *Asian J. Atmos. Environ.*, 18, 21, <https://doi.org/10.1007/s44273-024-00042-z>, 2024.
- Yamaga, S., Ban, S., Xu, M., Sakurai, T., Itahashi, S., and Matsuda, K.: Trends of sulfur and nitrogen deposition from 2003 to 2017 in Japanese remote areas, *Environ. Pollut.*, 289, 117842, <https://doi.org/10.1016/j.envpol.2021.117842>, 2021.
- Yamashita, N., Ohta, S., Sase, H., Kievuttinon, B., Luangjame, J., Visaratana, T., and Garivait, H.: Seasonal changes in multi-scale spatial structure of soil pH and related parameters along a tropical dry evergreen forest slope, *Geoderma*, 165(1), 31–39, <https://doi.org/10.1016/j.geoderma.2011.06.020>, 2011.
- Yamashita, N., Sase, H., and Kurokawa, J.: Assessing critical loads and exceedances for acidification and eutrophication in the forests of East and Southeast Asia: A comparison with EANET monitoring data, *Sci. Total Environ.*, 851, 158054, <https://doi.org/10.1016/j.scitotenv.2022.158054>, 2022.
- Zhang, L., Wright, L. P., & Asman, W. A. H.: Bi-directional air-surface exchange of atmospheric ammonia: A review of measurements and a development of a big-leaf model for applications in regional-scale air-quality models. *J. Geophys. Res. Atmos.*, 115(D20), D20310. <https://doi.org/10.1029/2009JD013589>, 2010
- Zhou, K., Xu, W., Zhang, L., Ma, M., Liu, X., and Zhao, Y.: Estimating nitrogen and sulfur deposition across China during 2005 to 2020 based on multiple statistical models, *Atmos. Chem. Phys.*, 23, 8531–8551, <https://doi.org/10.5194/acp-23-8531-2023>, 2023.